Quantum electronics

4

Magnetization reversal

IFM PAN
Maciej Urbaniak
Politechnika Poznańska 2018

Magnetization reversal

- Beyond Stoner-Wohlfarth model
- Landau-Lifshitz-Gilbert equation
- Micromagnetism

Landau-Lifshitz-Gilbert (LLG) equation of spin motion

- The change of angular momentum of a rigid body under the influence of the torque is given by:

$$\vec{\tau} = \frac{d\vec{J}}{dt}$$

- The torque acting on magnetic moment in magnetic field is: $\vec{\tau} = \vec{m} \times \vec{B}$
- With gyromagnetic ratio defined as $\gamma = \frac{|\vec{m}|}{|\vec{J}|}$ we get:

For an electron we have:

$$\vec{m}_e = -g_e \frac{e}{2m} \vec{S}$$

$$\frac{d\vec{m}}{dt} = \gamma\, \vec{m} \times \vec{B}$$

This equation can be used to describe motion of the electron's magnetic moment. The electron itself is fixed in space.

- Larmor precession [3]

Vector rotating with angular velocity Ω changes according to the formula:

$$\frac{d\vec{A}}{dt} = \vec{\Omega} \times \vec{A}$$

- From equation for time change of **m** we get:

$$\frac{d\vec{m}}{dt} = \gamma \vec{m} \times \vec{B} = -\gamma \vec{B} \times \vec{m} = -\omega_L \times \vec{m}$$

Landau-Lifshitz-Gilbert (LLG) equation of spin motion

- The velocity is called *Larmor angular velocity* and is given by:

$$\vec{\Omega}_L = \gamma \vec{B}$$

- The corresponding *Larmor frequency* is:

$$f_L = \frac{1}{2\pi} \gamma B$$

- For electron *Larmor frequency* is approximately 1.761×10^{11} rad $s^{-1}T^{-1}$ *

*http://physics.nist.gov/cgi-bin/cuu/Value?gammae retrieved 2012.05.16

Landau-Lifshitz-Gilbert (LLG) equation of spin motion

•Landau and Lifshitz have introduced **a damping term** to the precession equation:

$$\frac{d\vec{m}}{dt} = \gamma\,\vec{m}\times\vec{B} - \frac{\alpha_L}{|\vec{m}|}\left(\vec{m}\times\left(\vec{m}\times\vec{B}\right)\right), \qquad (1)$$

where α_L is a dimensionless parameter [5].

•As can be seen the damping vector $-\vec{m}\times(\vec{m}\times\vec{B})$ is directed toward ***B*** and vanishes when ***m*** and ***B*** become parallel.

•As can be seen from Eq. (1) the acceleration of ***m*** towards ***B*** is greater the higher the damping constant α_L. Gilbert [6] pointed out that this is nonphysical and that Eq. (1) can be used for small damping only [5].

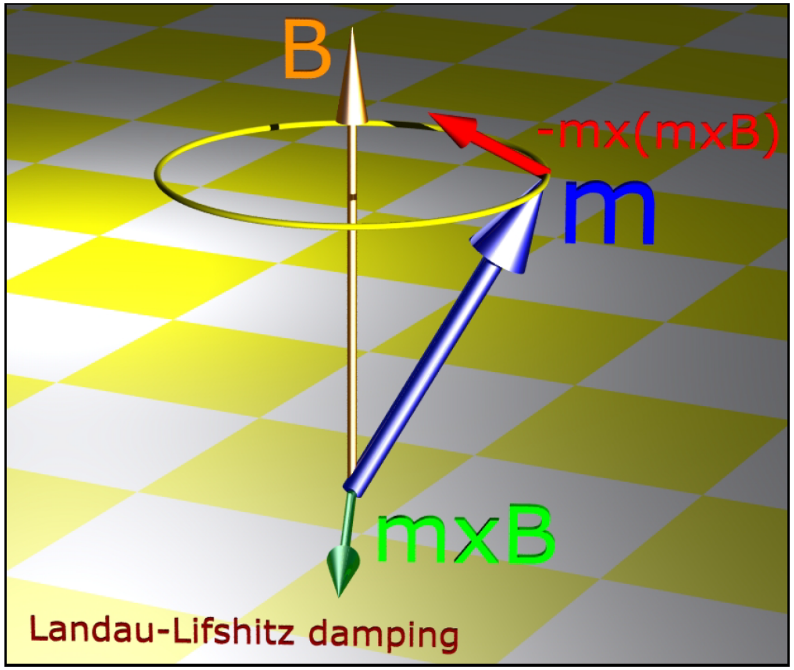

•He introduced other phenomenological form of equation which can be used for arbitrary damping. Damping is introduced as dissipative term [7] of the effective field acting on the moment:

$$\vec{B} \rightarrow \vec{B} - \eta\frac{d\vec{m}}{dt} \qquad (2)$$

Landau-Lifshitz-Gilbert (LLG) equation of spin motion

$$\frac{d\vec{m}}{dt}=\gamma\,\vec{m}\times\vec{B}$$
$$\vec{B}\rightarrow\vec{B}-\eta\frac{d\vec{m}}{dt}$$

- Inserting Eq. (2) into precession equation (3 slides back) we obtain:

$$\frac{d\vec{m}}{dt}=\gamma\,\vec{m}\times\vec{B}=\gamma\,\vec{m}\times\left(\vec{B}-\eta\frac{d\vec{m}}{dt}\right)=\gamma\,\vec{m}\times\vec{B}=\gamma\,\vec{m}\times\vec{B}-\gamma\,\eta\,\vec{m}\times\frac{d\vec{m}}{dt}=$$
$$\gamma\,\vec{m}\times\vec{B}-\frac{\alpha}{|\vec{m}|}\vec{m}\times\frac{d\vec{m}}{dt},\quad \text{with}\quad \alpha=\gamma\,\eta\,|\vec{m}|$$

- The equation can be transformed by substituting itself into righ-hand side:

$$\frac{d\vec{m}}{dt}=\gamma\,\vec{m}\times\vec{B}-\frac{\alpha}{|\vec{m}|}\vec{m}\times\frac{d\vec{m}}{dt}=\gamma\,\vec{m}\times\vec{B}-\frac{\alpha}{|\vec{m}|}\vec{m}\times\left(\gamma\,\vec{m}\times\vec{B}-\frac{\alpha}{|\vec{m}|}\vec{m}\times\frac{d\vec{m}}{dt}\right)$$

- Multiplying out we get:

$$\frac{d\vec{m}}{dt}=\gamma\,\vec{m}\times\vec{B}-\frac{\alpha\,\gamma}{|\vec{m}|}\vec{m}\times\vec{m}\times\vec{B}+\frac{\alpha^2}{|\vec{m}|^2}\vec{m}\times\vec{m}\times\frac{d\vec{m}}{dt}\qquad(3)$$

- Using vector identity $\vec{a}\times(\vec{b}\times\vec{c})=\vec{b}\,(\vec{a}\cdot\vec{c})-\vec{c}\,(\vec{a}\cdot\vec{b})$ we have:

$$\vec{m}\times\vec{m}\times\frac{d\vec{m}}{dt}=\vec{m}\,(\vec{m}\cdot\frac{d\vec{m}}{dt})-\frac{d\vec{m}}{dt}|\vec{m}|^2$$

- Since the magnitude of ***m*** is assumed to be constant* there can be no component of $\frac{d\vec{m}}{dt}$ which is parallel to ***m***; we get then:

$$\vec{m}\times\vec{m}\times\frac{d\vec{m}}{dt}=-\frac{d\vec{m}}{dt}|\vec{m}|^2\qquad(4)$$

*if the system consists of a number of individual moments, each of which is damped slightly differently, the magnitude of the total magnetic moment may not be conserved; one should use Bloch equation then.

Landau-Lifshitz-Gilbert (LLG) equation of spin motion

- Inserting Eq. (4) into Eq. (3) we obtain:

$$\frac{d\vec{m}}{dt}=\gamma\,\vec{m}\times\vec{B}-\frac{\alpha\,\gamma}{|\vec{m}|}\vec{m}\times\vec{m}\times\vec{B}-\alpha^2\frac{d\vec{m}}{dt}$$

$$\alpha=\gamma\,\eta|\vec{m}|$$

$$\frac{d\vec{m}}{dt}(1+\alpha^2)=\gamma\,\vec{m}\times\vec{B}-\frac{\alpha\,\gamma}{|\vec{m}|}\vec{m}\times\vec{m}\times\vec{B}$$

- And finally:

Landau-Lifshitz-Gilbert equation

$$\frac{d\vec{m}}{dt}=\frac{\gamma}{(1+\alpha^2)}\vec{m}\times\vec{B}-\frac{\alpha}{(1+\alpha^2)}\frac{\gamma}{|\vec{m}|}\vec{m}\times\vec{m}\times\vec{B}$$

- In general the magnetic induction should be replaced by the effective field ***B***$_{eff}$ [9, p. 178]:

$$\vec{B}_{eff}=\mu_0\left(\frac{C}{M^2}\left[(\nabla M_x)^2+(\nabla M_y)^2+(\nabla M_z)^2\right]+\vec{H}+\frac{\partial}{\partial\vec{m}}E_{anisotropy}\right)$$

exchange energy density – see later in the lecture

to be read as $\frac{\partial}{\partial\vec{m}}f=\hat{x}\frac{\partial}{\partial m_x}f+\hat{y}\frac{\partial}{\partial m_y}f+\hat{z}\frac{\partial}{\partial m_z}f$ [9, p.178]

Landau-Lifshitz-Gilbert (LLG) equation of spin motion

Landau-Lifshitz-Gilbert equation

$$\frac{d\vec{m}}{dt}=\frac{\gamma_G}{(1+\alpha_G^2)}\vec{m}\times\vec{B}-\frac{\alpha_G}{(1+\alpha_G^2)}\frac{\gamma_G}{|\vec{m}|}\vec{m}\times\vec{m}\times\vec{B}$$

Landau-Lifshitz equation

$$\frac{d\vec{m}}{dt}=\gamma_L\vec{m}\times\vec{B}-\frac{\alpha_L}{|\vec{m}|}(\vec{m}\times(\vec{m}\times\vec{B}))$$

•With the replacement $\gamma_L=\frac{\gamma_G}{1+\alpha_G^2}$, $\alpha_L=\frac{\alpha_G\gamma_G}{1+\alpha_G^2}$ both equations have similar form but...

the dependencies of precessional and relaxation terms on damping constant are quite different [8]:

•According to LL equation the relaxation becomes faster with increasing damping α_L (red dashed curve) which is counter intuitive.

•In case of LLG equation the behavior of both terms agree with the expectations for the dynamics of damped precession [8].

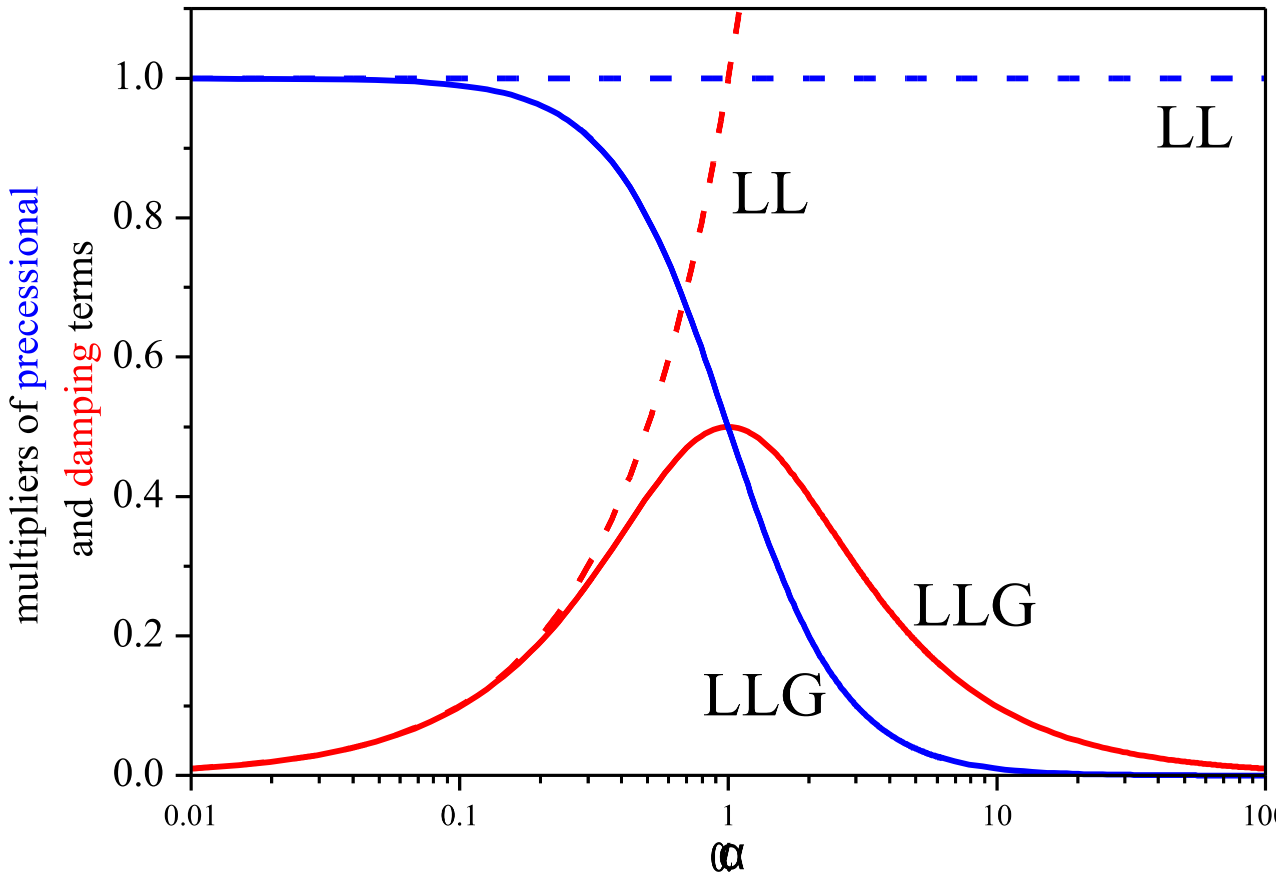

Magnetic moment reversal

- Let us consider the LLG equation describing the orientation of a single moment (monodomain state) of magnetized sphere fixed in space (no translational motion):

$$\frac{d\vec{M}}{dt}=\frac{\gamma\mu_0}{(1+\alpha^2)}\left(\vec{M}\times\vec{H}-\frac{\alpha}{M}\left[\vec{M}\times(\vec{M}\times\vec{H})\right]\right)$$

- For simplicity the time scale is changed: $\tau=\frac{t\,M\,\gamma\,\mu_0}{(1+a^2)}$

$$M^2\frac{d\vec{M}}{d\tau}=M\,\vec{M}\times\vec{H}-\alpha\left[\vec{M}\times(\vec{M}\times\vec{H})\right]$$

- We assume that the external field is applied along z-direction [$\boldsymbol{B}_a/\mu_0=(0,0,H_z)$]. The demagnetizing field inside the sphere is ($H_d=-1/3\ H_z$). With $\boldsymbol{H}=\boldsymbol{H}_a-\boldsymbol{H}_d$ we obtain:

$$M^2\frac{dM_x}{d\tau}=-\alpha H_z M_x M_z+H_z M_y M$$

$$M^2\frac{dM_y}{d\tau}=-\alpha H_z M_y M_z-H_z M_x M$$

$$M^2\frac{dM_z}{d\tau}=\alpha\left(H_z M_x^2+H_z M_y^2\right)$$

- Verifying that d$\boldsymbol{M}$ is perpendicular to $\boldsymbol{M}$ $[(dM_x, dM_y, dM_z)\cdot\vec{M}=0]$ we see that the length of the magnetization is preserved as expected.

(-α Hz Mx Mz +Hz My M,-α Hz My Mz -Hz Mx M, α (Hz Mx Mx +Hz My My)).(Mx,My,Mz)=0

Ryoichi Kikuchi, J. Appl. Phys. 27, 1352 (1956)

Magnetic moment reversal

- We can then rewrite the equation for M_z obtaining the equation of motion that does not depend on M_x and M_y:

$$M^2 \frac{dM_z}{d\tau} = \alpha H_z (M^2 - M_z^2) \xleftarrow{|\vec{M}|=const} M^2 \frac{dM_z}{d\tau} = \alpha (H_z M_x^2 + H_z M_y^2)$$

- Integrating between the final and the initial values of M_z we have:

$$\alpha H_z \tau = \int_{M_z^i}^{M_z^f} \frac{M^2}{(M^2 - M_z^2)} dM_z = M\, ArcTanh\left[\frac{M_z}{M}\right]_{M_z^i}^{M_z^f} = M \ln \left| \frac{\sqrt{-1 - M_z/M}}{\sqrt{-1 + M_z/M}} \right|_{M_z^i}^{M_z^f} =$$

$$M\left(\ln\left|\sqrt{\frac{-1 - M_z^f/M}{-1 + M_z^f/M}}\right| - \ln\left|\sqrt{\frac{-1 - M_z^i/M}{-1 + M_z^i/M}}\right| \right) = M\left(\ln\left|\sqrt{\frac{-1 - M_z^f/M}{-1 + M_z^f/M}\,\frac{-1 + M_z^i/M}{-1 - M_z^i/M}}\right| \right) =$$

$$\frac{1}{2} M \ln\left|\frac{(M + M_z^f)(M - M_z^i)}{(M - M_z^f)(M + M_z^i)}\right|$$

- Going back to the actual time we get for the time for M_z to change from the initial to final value:

$$\tau = \frac{t M \gamma \mu_0}{(1 + a^2)}$$

$$\boxed{t_F = \frac{1}{2\gamma H_z} \frac{1 + \alpha^2}{\alpha} \ln\left|\frac{(M + M_z^f)(M - M_z^i)}{(M - M_z^f)(M + M_z^i)}\right|}$$

Ryoichi Kikuchi, J. Appl. Phys. 27, 1352 (1956)

Magnetic moment reversal

$$t_F = \frac{1}{2\gamma H_z}\frac{1+\alpha^2}{\alpha}\ln\left|\frac{\left(M+M_z^f\right)\left(M-M_z^i\right)}{\left(M-M_z^f\right)\left(M+M_z^i\right)}\right|$$

- If at t=0 the magnetization/moment points exactly along z-axis (M_z=-M) then t_F would be infinite – **no switching**.
- If there is no damping (α=0) then t_F would be infinite – the moment of the sample would precess around the external field direction.

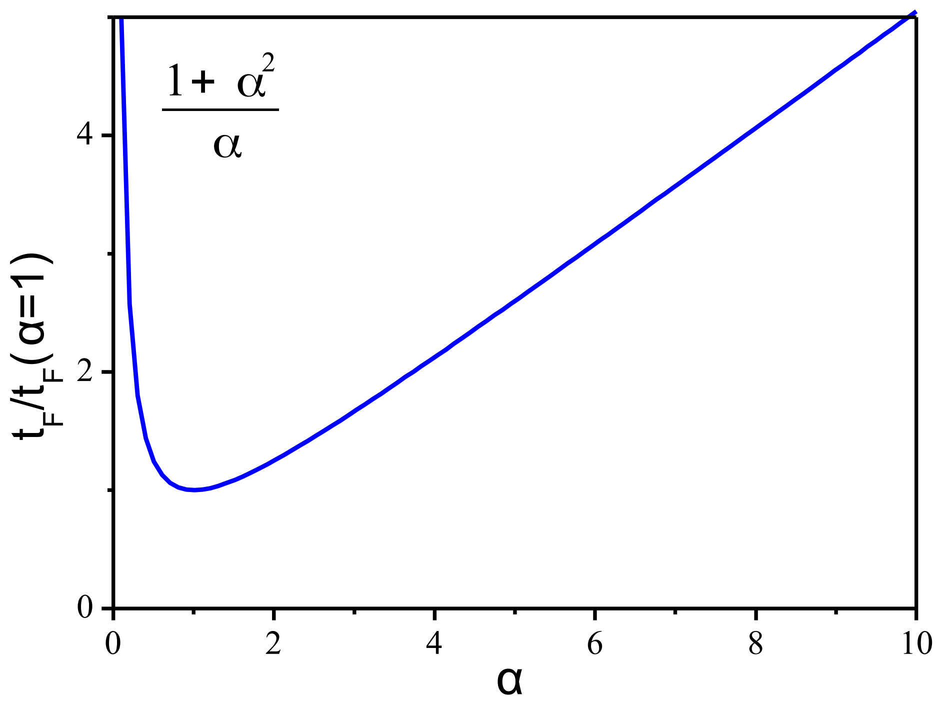

- The shortest switching time is obtained for finite value of damping coefficient (α=1).
- The value of the critical damping constant depends on the shape of the sample.
- For single domain thin film the critical α is about 0.013.
- For permalloy films the minimum switching time, as obtained from the similar calculations is about **1 ns**.

Ryoichi Kikuchi, J. Appl. Phys. 27, 1352 (1956)

Magnetic moment reversal

- Time evolution of magnetic moment orientation for low and high damping:
  - initial orientation of magnetic moment: (0,0.001,1)
  - magnetic field instantaneously switched on to value: (0,0,-1)

H||**z** axis

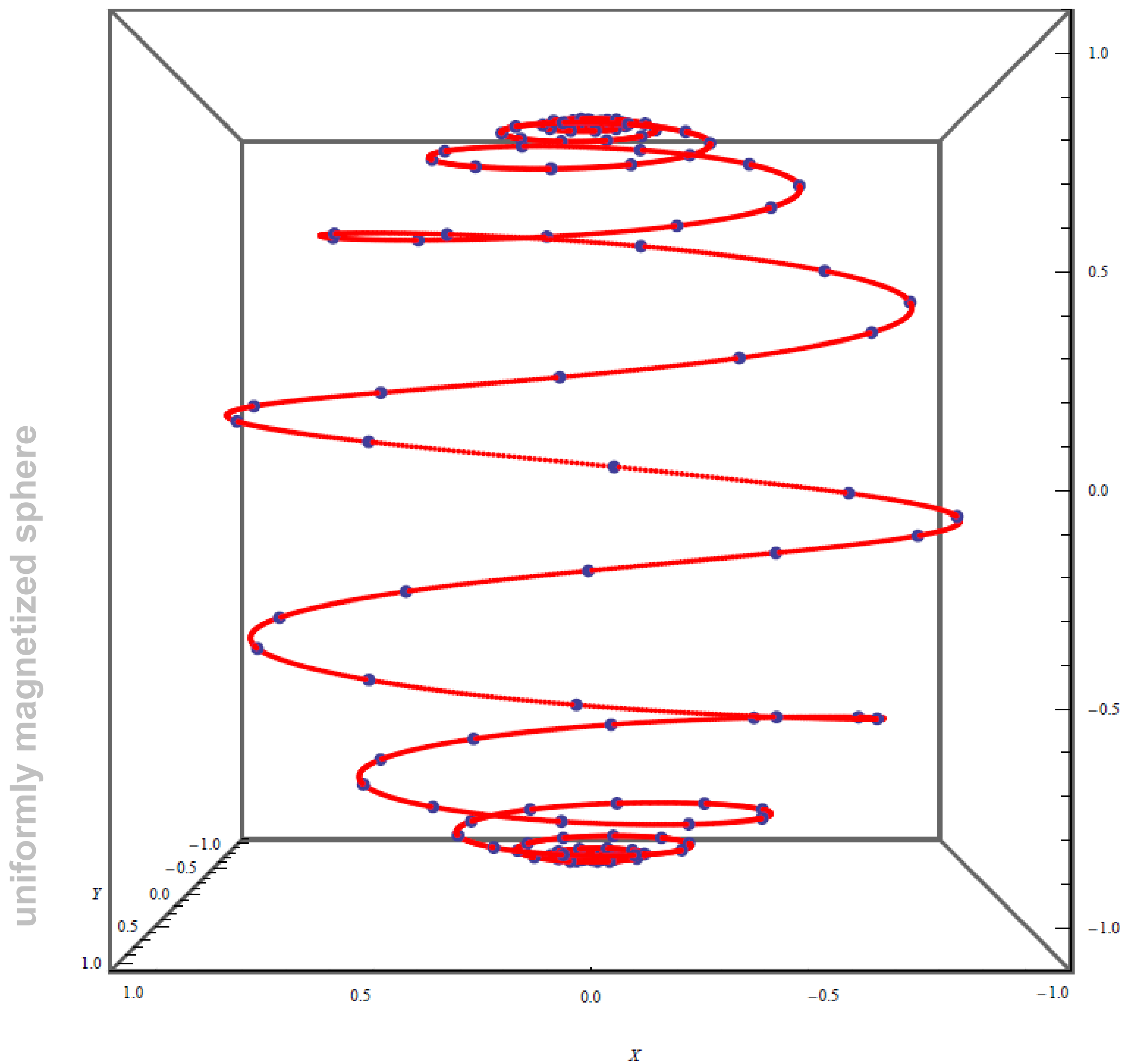

- **α=0.1**
- **blue dots** mark the same time intervals
- the end of moment moves from top to bottom

Wolfram Mathematica 6.0 code to obtain these curves:

```
ilepunktow=9000;
orientacjamomentu=Table[{0,0,0},{i,1,ilepunktow-1}];
dt=0.025;
alfa=0.1;
Hz=-1;
Mi={0,0.001,1};(*initial moment orientation*)
moment=Sqrt[Mi.Mi];(*moment's length*)
licznik=0;
gamma=2;
timemultiplier=1/(moment gamma (1+alfa^2));

coile=50;(*co ile punktow stawiac marker*)
macierzznacznikow=Table[{0,0,0},{i,1,Floor[ilepunktow/coile]-1}];
licznik=1;
l=1;
For[k=1,k<ilepunktow,k++,

Mi[[1]]=Mi[[1]]+dt timemultiplier  Hz(moment Mi[[2]] -alfa Mi[[1]] Mi[[3]])/moment^2;
Mi[[2]]=Mi[[2]]+dt timemultiplier  Hz(-moment Mi[[1]] -alfa Mi[[2]] Mi[[3]])/moment^2;
Mi[[3]]=Mi[[3]]+dt timemultiplier Hz alfa (Mi[[1]]^2+ Mi[[2]]^2)/moment^2;
orientacjamomentu[[k,1]]=Mi[[1]];orientacjamomentu[[k,2]]=Mi[[2]];orientacjamomentu[[k,3]]=Mi[[3]];

(*matrix of markers*)
If[licznik<coile,licznik=licznik+1,{licznik=1;
macierzznacznikow[[l,1]]=orientacjamomentu[[k,1]];
macierzznacznikow[[l,2]]=orientacjamomentu[[k,2]];
macierzznacznikow[[l,3]]=orientacjamomentu[[k,3]];

l++}
]

]
wy1=ListPointPlot3D[orientacjamomentu, PlotRange->{{-1.1,1.1},{-1.1,1.1},{-1.1,1.1}},
BoxRatios->{1,1,1},PlotStyle->{Red},AxesLabel->{X,Y,Z},ViewPoint->{0,Pi,0},BoxStyle->Directive[Thickness[0.004]]];

wy4=ListPointPlot3D[macierzznacznikow, PlotRange->{{-1.1,1.1},{-1.1,1.1},{-1.1,1.1}},
BoxRatios->{1,1,1},PlotStyle->PointSize[Large],AxesLabel->{X,Y,Z},ImageSize->600,ViewPoint->{Pi,Pi/2,2}];
wy2=Graphics3D[{Opacity[0.5],Sphere[{0,0,0},1]}];
wy3=Graphics3D[{AbsoluteThickness[2],Line[{{0,0,0},{0,0,1}}]}];
wy3=Show[wy1,wy2,wy3,wy4,ImageSize->600,ViewPoint->{Pi,Pi/2,2},ImageMargins->20]
```

Ryoichi Kikuchi, J. Appl. Phys. 27, 1352 (1956)

Magnetic moment reversal

- Time evolution of magnetic moment orientation for low and high damping:
  - initial orientation of magnetic moment: (0,0.001,1)
  - magnetic field instantaneously switched on to value: (0,0,-1)

H||***z*** axis

uniformly magnetized sphere

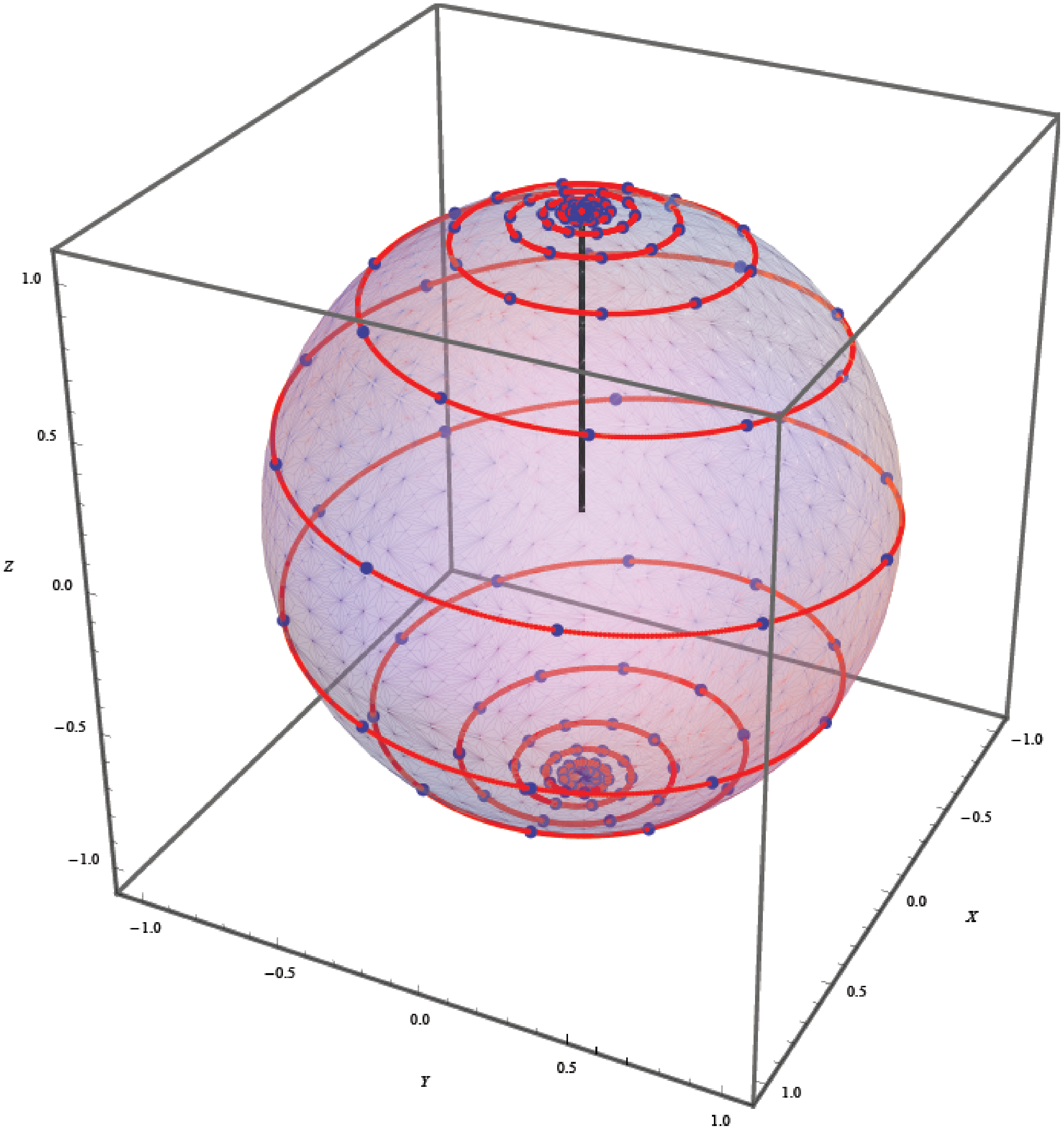

- **α=0.1**
- **blue dots** mark the same time intervals
- the end of moment moves from top to bottom

Ryoichi Kikuchi, J. Appl. Phys. 27, 1352 (1956)

Magnetic moment reversal

- Time evolution of magnetic moment orientation for low and high damping:
  - initial orientation of magnetic moment: (0,0.001,1)
  - magnetic field instantaneously switched on to value: (0,0,-1)

H||***z*** axis

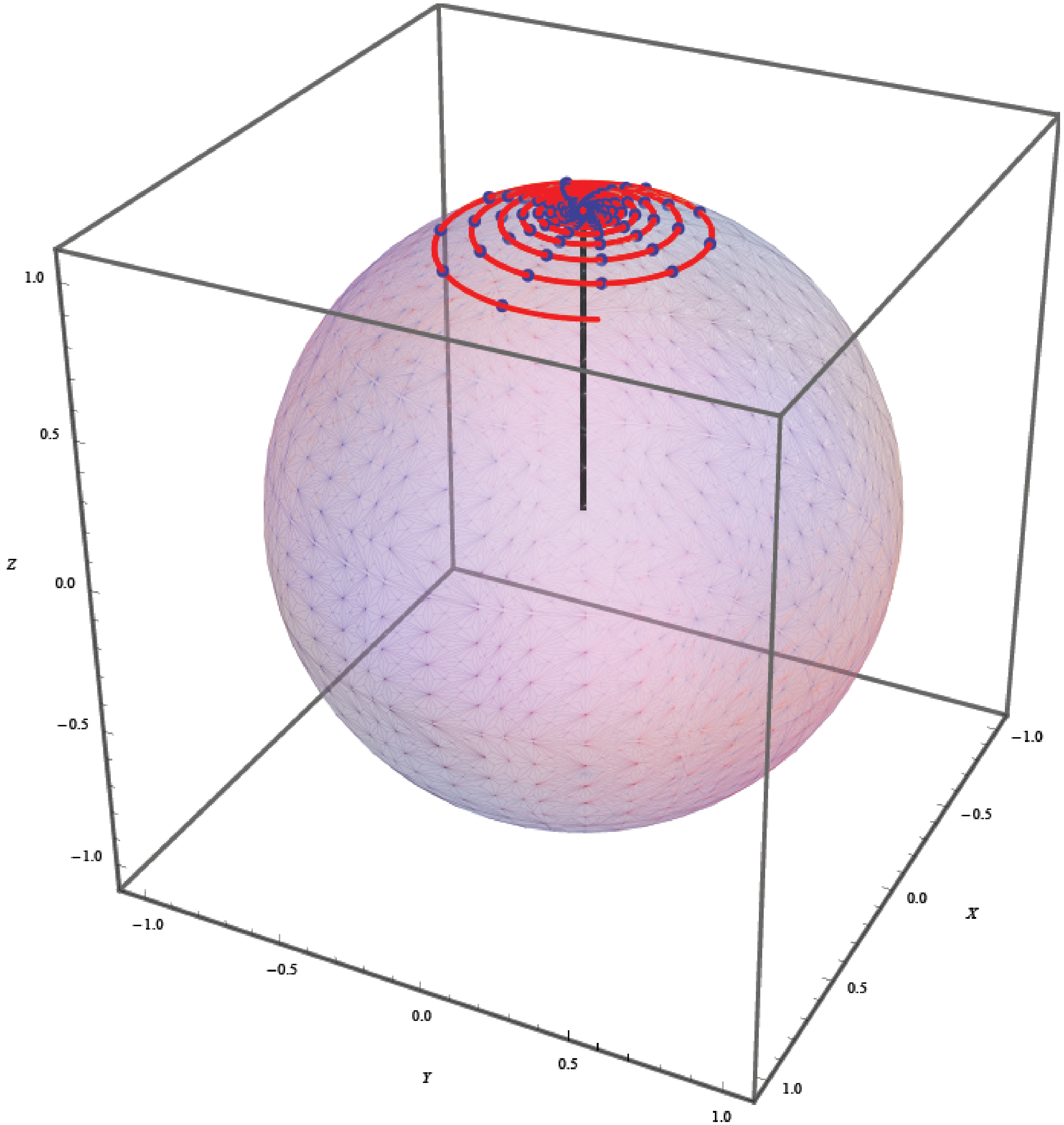

uniformly magnetized sphere

- **α=0.05**
- **blue dots** mark the same time intervals
- the end of moment moves from top to bottom
- the total time of movement is the same as on the previous page
- note that due to weaker damping the moment did not change its orientation to *-z* – **the switching is delayed**

Ryoichi Kikuchi, J. Appl. Phys. 27, 1352 (1956)

Magnetic moment reversal

•Time evolution of magnetic moment orientation for low and high damping:
➢initial orientation of magnetic moment: (0,0.001,1)
➢magnetic field instantaneously switched on to value: (0,0,-1)

H||***z*** axis

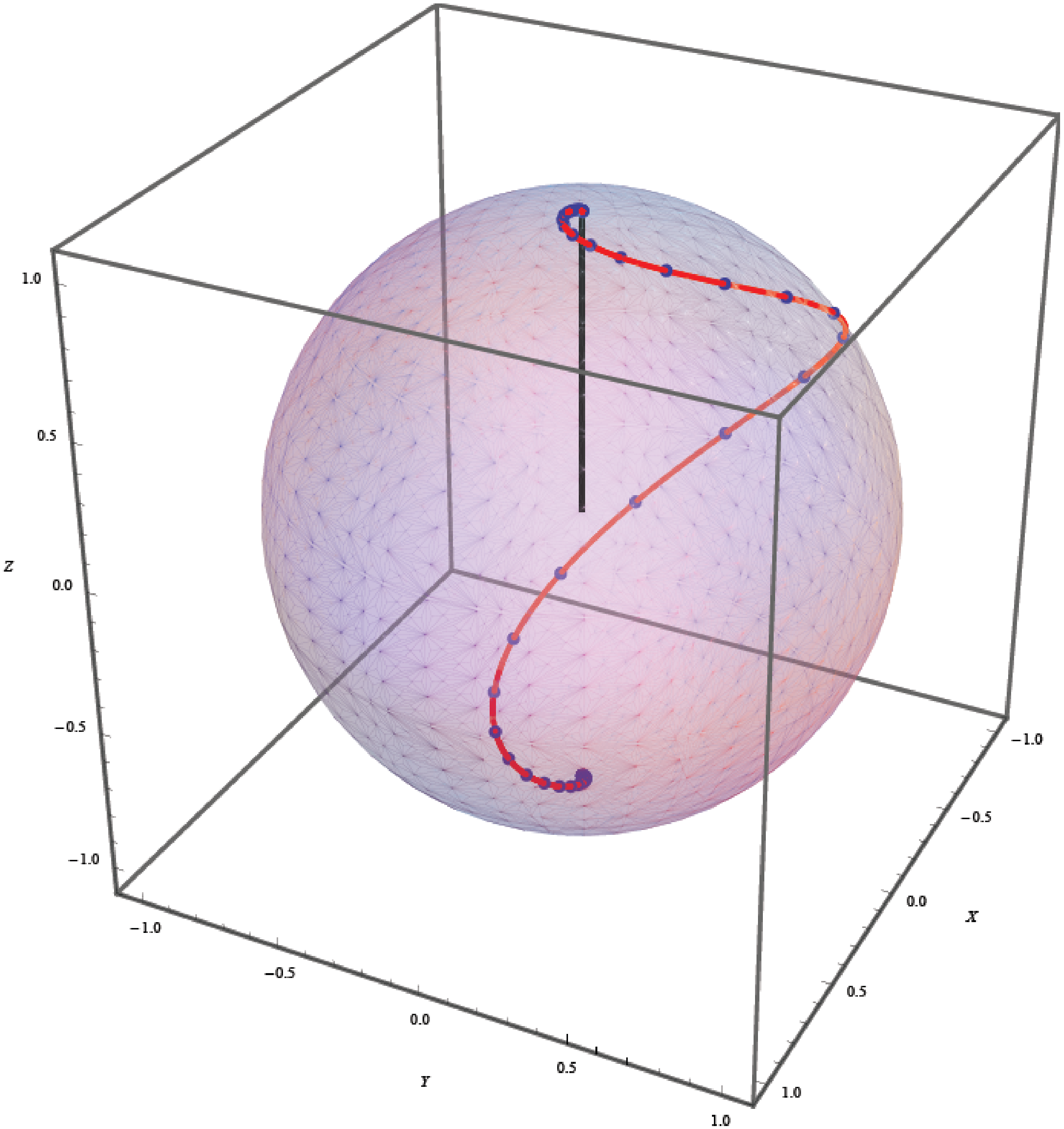

uniformly magnetized sphere

•**α=1** – **minimal switching time**

•**blue dots** mark the same time intervals

•the end of moment moves from top to bottom

Ryoichi Kikuchi, J. Appl. Phys. 27, 1352 (1956)

Magnetic moment reversal

- Note that further increase of damping constant α slows down the switching of magnetic moment (more blue dots)

•α=1 – **minimal switching time**

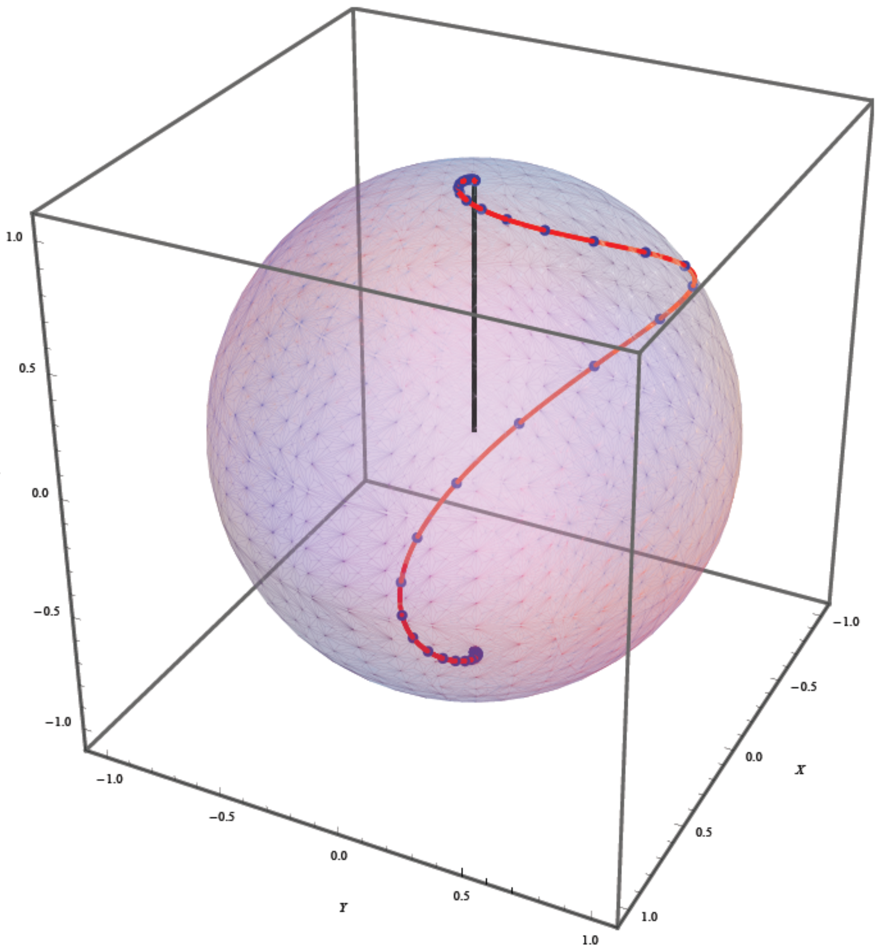

•α=10

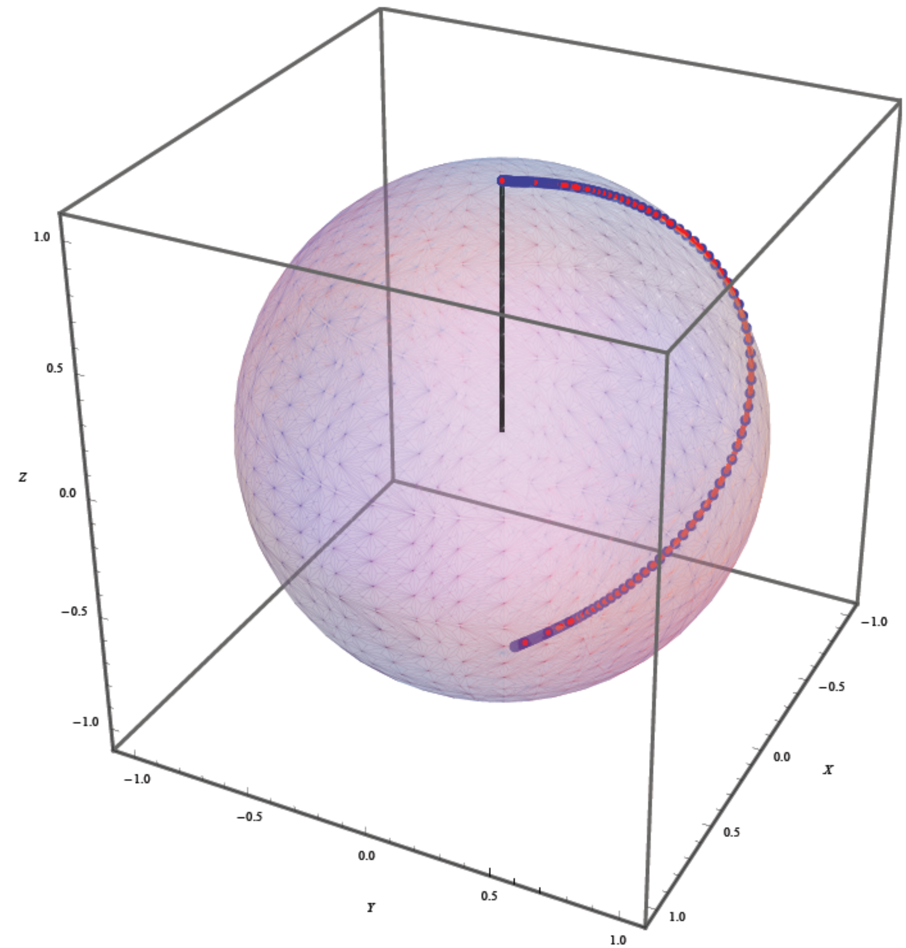

uniformly magnetized sphere

Ryoichi Kikuchi, J. Appl. Phys. 27, 1352 (1956)

Magnetic moment reversal – thin film

- Time evolution of magnetic moment orientation for low and high damping:
  - initial orientation of magnetic moment: (-1,0.001,0) – in plane of the sample
  - magnetic field instantaneously switched on to value: (+1,0,0)

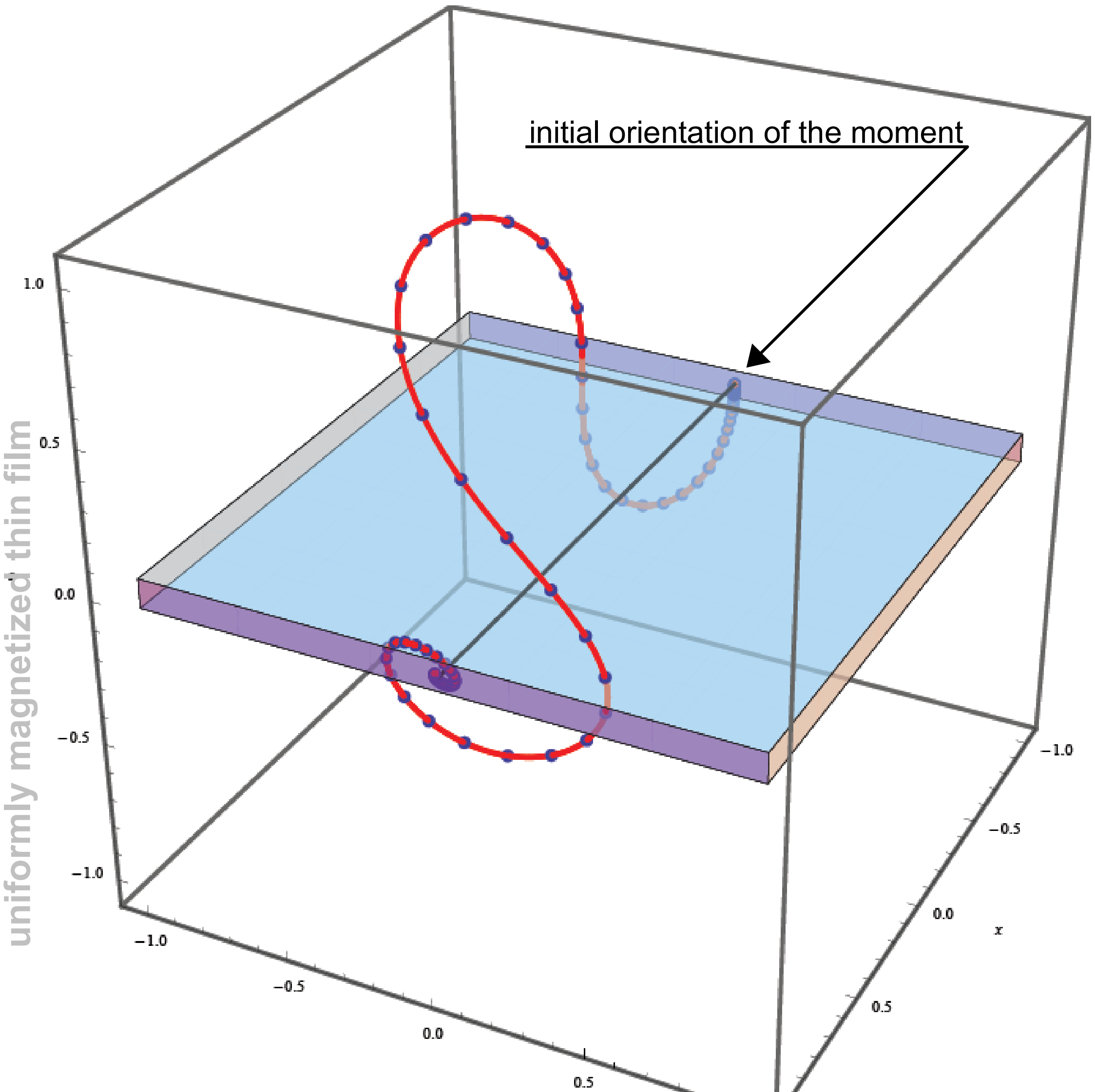

- **α=0**
- the end of moment moves from behind to the front
- **blue dots** mark the same time intervals
- in thin films, contrary to the case of the single domain sphere, the demagnetizing field is, in general*, not parallel to magnetic moment and exerts a torque on it ⇒ the switching time depends on the magnetization
- for large α:

$$t_F \propto \frac{\alpha}{M}$$

$$\vec{H}_{demag} = -\hat{z} M_z$$

*it is parallel when ***M*** is along the film normal

Ryoichi Kikuchi, J. Appl. Phys. 27, 1352 (1956)

Magnetic moment reversal – thin film

- Time evolution of magnetic moment orientation for low and high damping:
  - initial orientation of magnetic moment: (-1,0.001,0) – in plane of the sample
  - magnetic field instantaneously switched on to value: (+1,0,0)

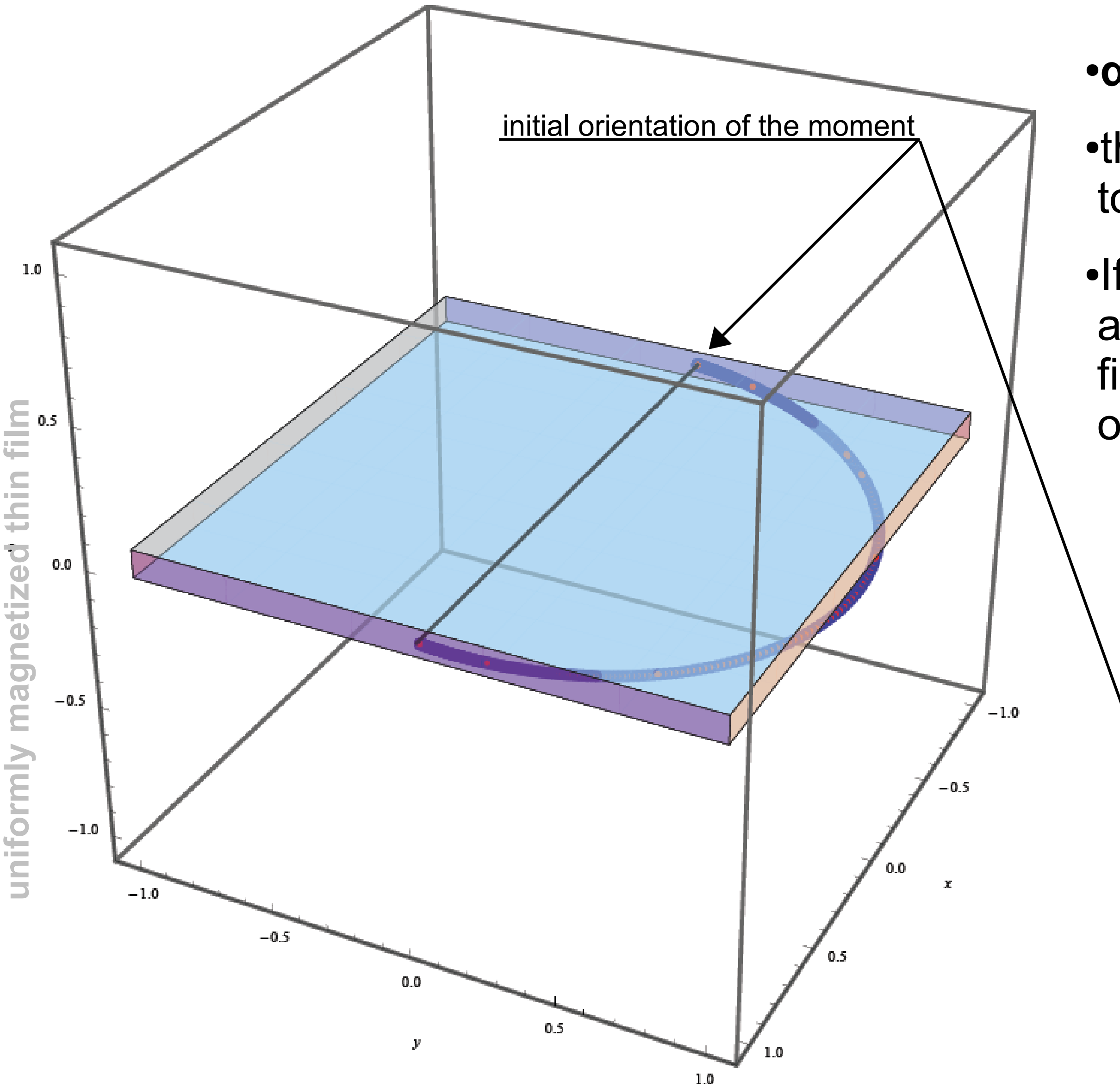

- **α=10**
- the end of moment moves from behind to the front
- If damping is high the moment rotates almost within **xy plane** and approaches field directions monotonically without oscillations

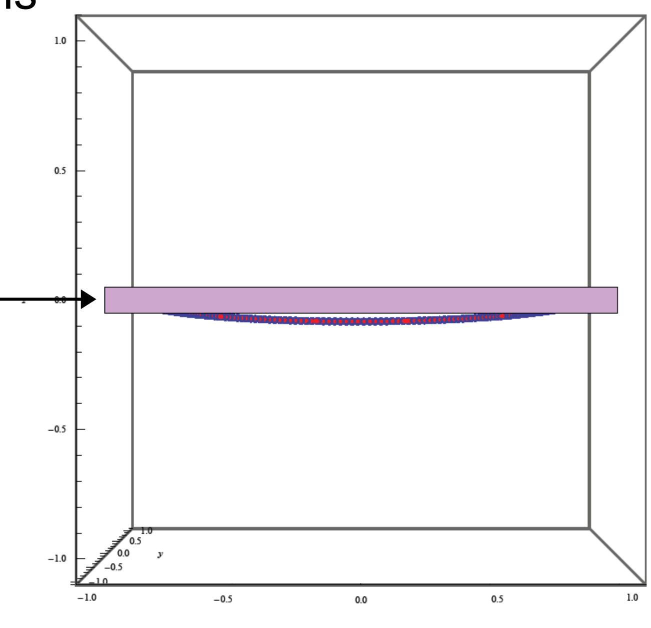

Ryoichi Kikuchi, J. Appl. Phys. 27, 1352 (1956)

Magnetic moment reversal – approach to saturation

- Trajectory of the moment depends on the field value:
  - initial orientation of magnetic moment: (-1,0.001,0) – in plane of the sample
  - magnetic field instantaneously switched on to value: (+1,0,0) (red line) or (+3,0,0) (**green** line)

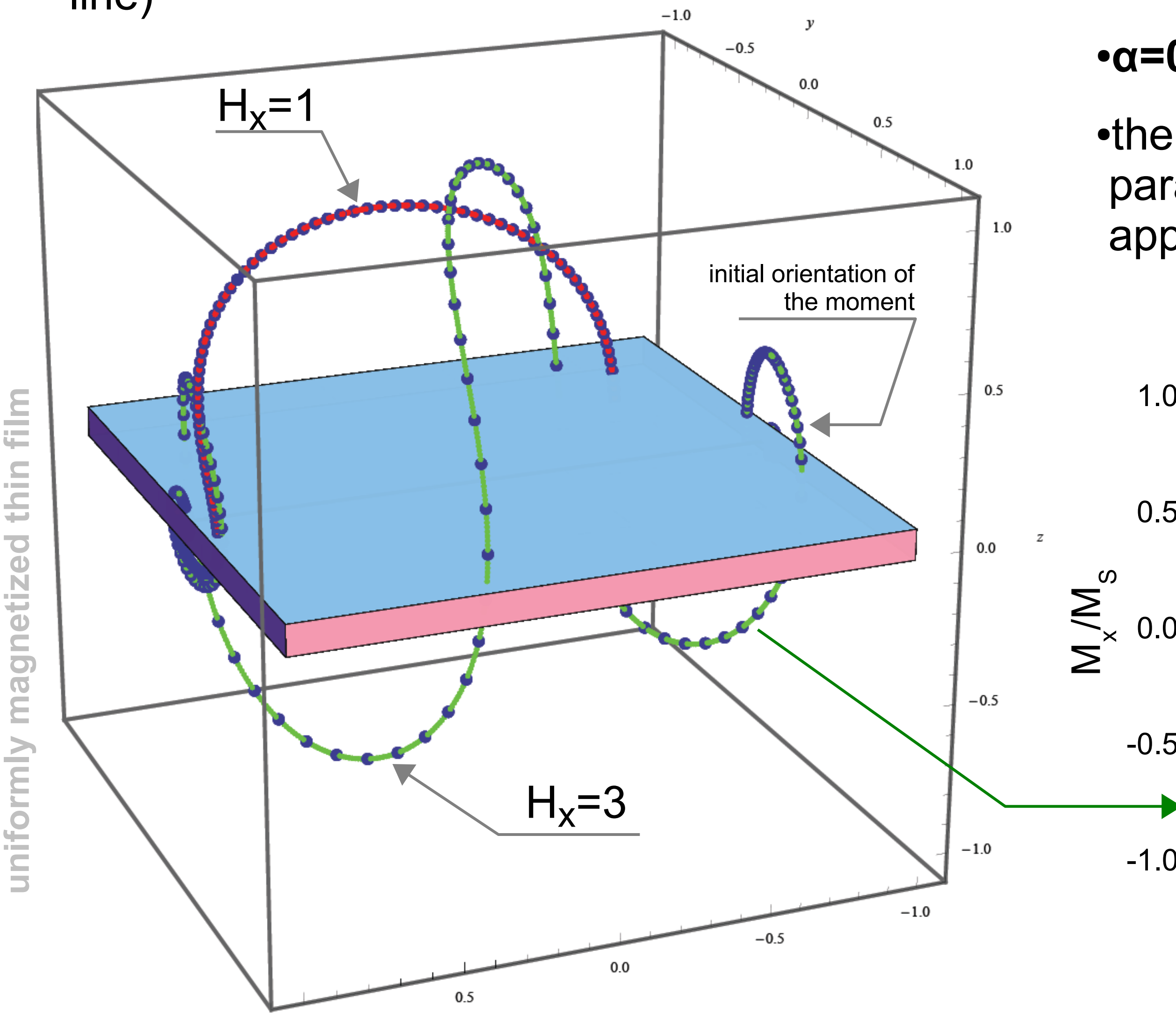

- **α=0.009**
- the component of magnetization parallel to the external field oscillatorilly approaches saturation

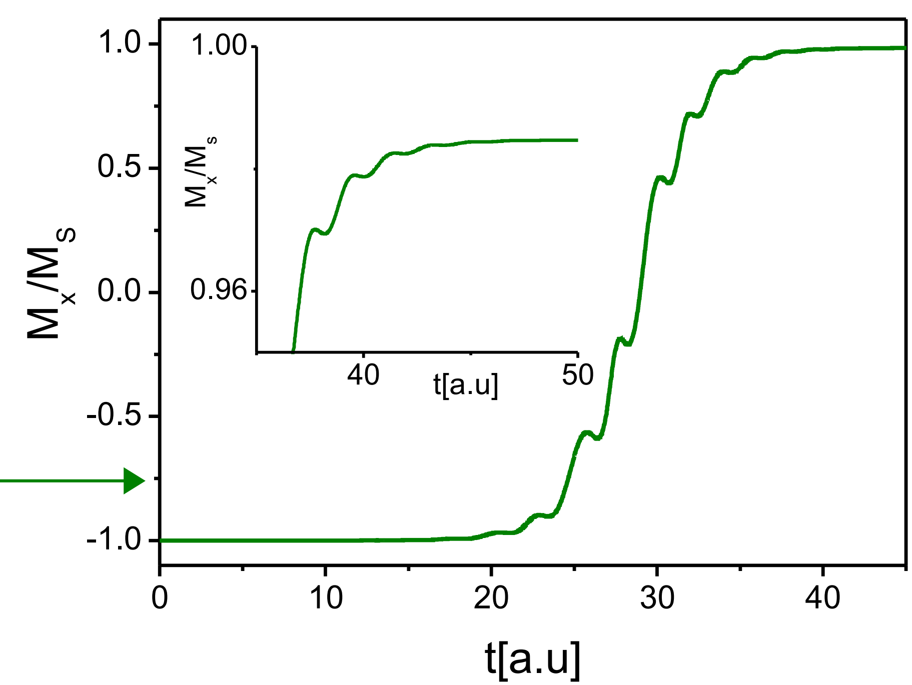

blue dots mark the same time intervals

Ryoichi Kikuchi, J. Appl. Phys. 27, 1352 (1956)

Element-resolved precessional dynamics

- Sputtered, 0.35 mm wide Cu(75nm)/Py(25nm)/Cu(3nm) trilayer
- Current pulses through thick Cu layer (10ns duration) create field pulses (Oersted field) perpendicular to the film stripline (in plane of the film)
- A bias field H_b can be applied parallel to the stripline in order to align the initial magnetization prior to excitation.
- **Element-selective** x-ray resonant magnetic scattering (XRMS)

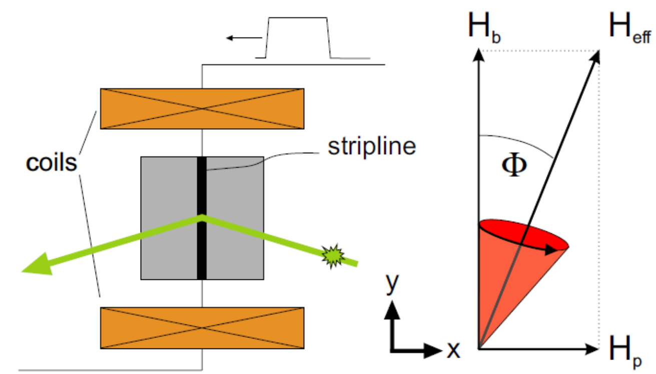

Figure 1. Schematic of the setup and fields applied at the sample region. The 350 μm stripline is centred on a Si substrate and oriented perpendicular to the scattering plane. A pair of coils provides the bias field H_b along the y-axis, the pulse field from the stripline is parallel to the x-axis. With our setup the change in the M_x-component is measured while the magnetization precesses around the effective field direction H_{eff}.

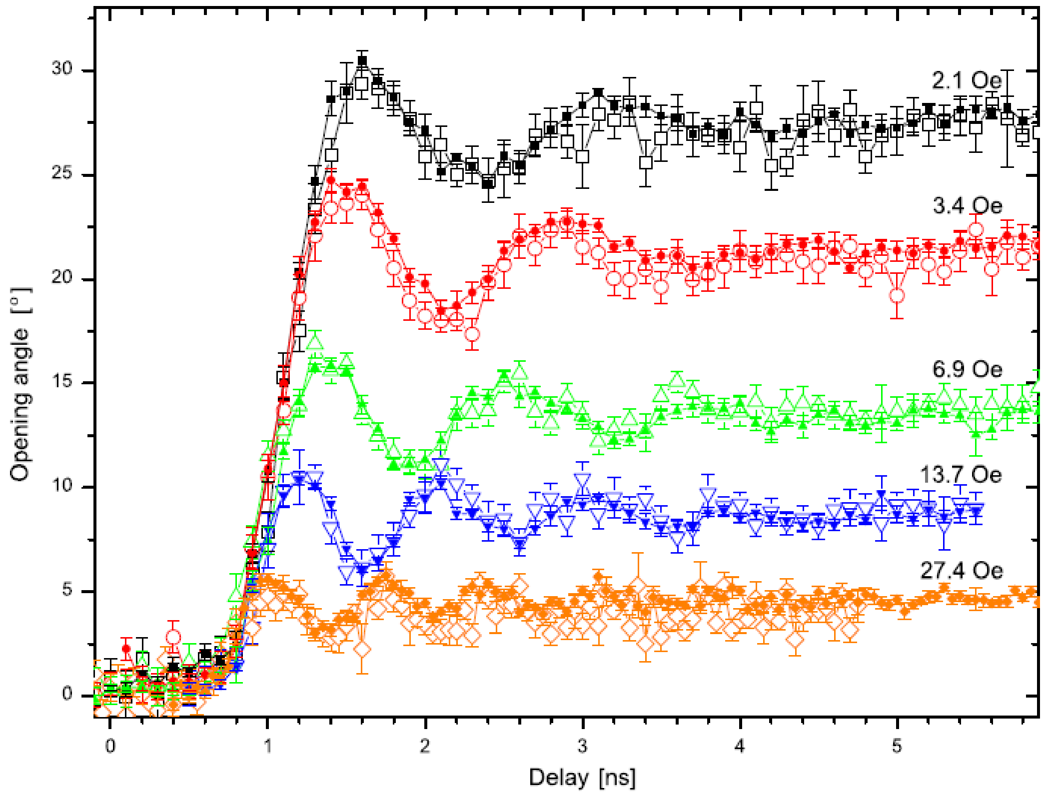

authors' “data show that Fe and Ni moments are aligned parallel to each other at all times, while they oscillate around the effective field direction given by the step field pulse and applied bias field”

Figure **5**. Comparison of the magnetization dynamics measured at the **Fe** (full) and **Ni** (open symbols) resonant edges for a set of different bias fields. The detected intensity is converted into opening angle φ according to the hysteresis curves.

S. Buschhorn, F. Brüssing, R. Abrudan and H. Zabel, J. Phys. D: Appl. Phys. **44** ,165001 (2011)

Spin coupling

The magnetic interactions between magnetic ions in a solid depend on numerous factors (neighboring ions, temperature, external fields etc.)
In some case to describe the system one uses Hamiltonian involving simultaneous interaction between several spins [10,11]:

$$E_{4s} = -\sum_{ijkl} K_{ijkl}\left[(\vec{S}_i\cdot\vec{S}_j)(\vec{S}_k\cdot\vec{S}_l) + (\vec{S}_i\cdot\vec{S}_l)(\vec{S}_j\cdot\vec{S}_k) - (\vec{S}_i\cdot\vec{S}_k)(\vec{S}_j\cdot\vec{S}_l)\right]$$

the energy term involves orientations of all four spin

In some other cases it is not enough to use bilinear forms* and biquadratic forms are introduced in addition

$$E_{4s} = -\sum_{ij} K_{ij}(\vec{S}_i\cdot\vec{S}_j)^2$$

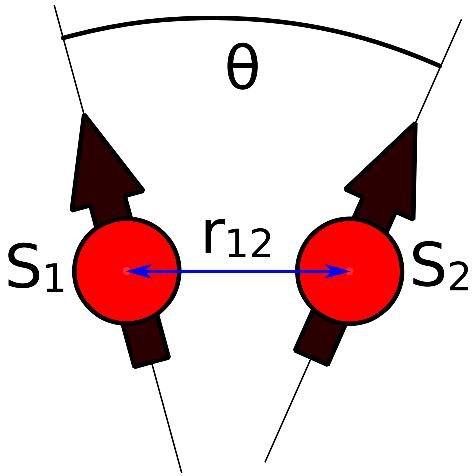

In most relevant cases however it is enough to use only **two spin terms that are bilinear** [13]

$$E_{bilinear} = -\sum_{ij} K_{ij} S_1^i S_2^j = K_{xx} S_1^x S_2^x + K_{xy} S_1^x S_2^y + \ldots$$

K_{ij} is a coupling 3×3 matrix, and in matrix notation we have

$$E_{bilinear} = \vec{S}_1 [K] \vec{S}_2$$

*"Form refers to a polynomial function in several variables where each term in the polynomial has the same degree. The degree of the term is the sum of the exponents." - K.C Border [12]

Spin coupling

The interaction matrix, like any 3×3 matrix [13], may be decomposed into a multiple of the identity matrix, an antisymmetric part (three different coefficients), and traceless* symmetric part:

$$K_{ij}=\begin{bmatrix} K_{11} & K_{12} & K_{13} \\ K_{21} & K_{22} & K_{23} \\ K_{31} & K_{32} & K_{33} \end{bmatrix}=J\begin{bmatrix} 1 & 0 & 0 \\ 0 & 1 & 0 \\ 0 & 0 & 1 \end{bmatrix}+\begin{bmatrix} 0 & D_1 & D_2 \\ -D_1 & 0 & D_3 \\ -D_2 & -D_3 & 0 \end{bmatrix}+\begin{bmatrix} A_1 & A_4 & A_5 \\ A_4 & A_2 & A_6 \\ A_5 & A_6 & A_3 \end{bmatrix}$$

$$J\vec{S}_1\begin{bmatrix} 1 & 0 & 0 \\ 0 & 1 & 0 \\ 0 & 0 & 1 \end{bmatrix}\vec{S}_2=S_1^x S_2^x+S_1^y S_2^y+S_1^z S_2^z=J\vec{S}_1\cdot\vec{S}_2$$

exchange coupling

$$E_{bilinear}=\vec{S}_1[K]\vec{S}_2$$

$$\vec{S}_1\begin{bmatrix} 0 & D_1 & D_2 \\ -D_1 & 0 & D_3 \\ -D_2 & -D_3 & 0 \end{bmatrix}\vec{S}_2=-D_1 S_1^y S_2^x-D_2 S_1^z S_2^x+D_1 S_1^x S_2^y-D_3 S_1^z S_2^y+D_2 S_1^x S_2^z+D_3 S_1^y S_2^z$$

$$=D_1(S_1^x S_2^y-S_1^y S_2^x)-D_2(S_1^z S_2^x-S_1^x S_2^z)+D_3(S_1^y S_2^z-S_1^z S_2^y)$$

$$=(\hat{i}D_3,-\hat{j}D_2,\hat{k}D_1)\cdot\vec{S}_1\times\vec{S}_2=\vec{D}\cdot(\vec{S}_1\times\vec{S}_2)$$

Dzyaloshinskii-Moriya interaction

*trace of a matrix – a sum of diagonal elements

Spin coupling

The interaction matrix, like any 3×3 matrix [13], may be decomposed into a multiple of the identity matrix, an antisymmetric part (three different coefficients), and traceless* symmetric part:

$$K_{ij}=\begin{bmatrix} K_{11} & K_{12} & K_{13} \\ K_{21} & K_{22} & K_{23} \\ K_{31} & K_{32} & K_{33} \end{bmatrix}=J\begin{bmatrix} 1 & 0 & 0 \\ 0 & 1 & 0 \\ 0 & 0 & 1 \end{bmatrix}+\begin{bmatrix} 0 & D_1 & D_2 \\ -D_1 & 0 & D_3 \\ -D_2 & -D_3 & 0 \end{bmatrix}+\begin{bmatrix} A_1 & A_4 & A_5 \\ A_4 & A_2 & A_6 \\ A_5 & A_6 & A_3 \end{bmatrix}$$

The matrix of the dipole-dipole interaction

$$E_{dipole-dipole}=\frac{-\mu_0}{4\pi|r|^3}\left[3(\hat{r}_{12}\cdot\vec{S}_1)(\hat{r}_{12}\cdot\vec{S}_2)-\vec{S}_1\cdot\vec{S}_2\right],$$

$\hat{r}_{12}$ - unit vector along the vector connecting two spins

reads

$$M_{dipole-dipole}=\frac{-\mu_0}{4\pi|r|^3}\begin{bmatrix} 3\hat{r}_x^2-1 & 3\hat{r}_x\hat{r}_y & 3\hat{r}_x\hat{r}_z \\ 3\hat{r}_x\hat{r}_y & 3\hat{r}_y^2-1 & 3\hat{r}_y\hat{r}_z \\ 3\hat{r}_x\hat{r}_z & 3\hat{r}_y\hat{r}_z & 3\hat{r}_z^2-1 \end{bmatrix}, \qquad \hat{r}_x^2+\hat{r}_y^2+\hat{r}_z^2=1$$

symmetric, traceless

Mathematica 9.0.1.0 code to get dipole-dipole matrix:

```
n =3;
wer={"x","y","z"};
r =Table[ ToExpression [StringJoin ["r",wer[[ i]]]],{i,1,n}];
S1 =Table[ ToExpression [StringJoin ["S1",wer[[ i]]]],{i,1,n}];
S2 =Table[ ToExpression [StringJoin ["S2",wer[[ i]]]],{i,1,n}];
macierz=Table[ToExpression[StringJoin["S1", wer[[i]],"*S2",wer[[j]]]],{i,1,n},
{j,1,n}];
m= Expand[ 3( r.S1)( r.S2)-S1.S2];(*write in here the spin hamiltonian (two
spin interaction), example dipole-dipole:
m= Expand[ 3( r.S1)( r.S2)-S1.S2];
*)
macierz2 =Table [Coefficient [m,macierz[[ i,j]]],{i,1,n},{j,1,n}] ;(*macierz2 is
the interaction matrix*)
TraditionalForm[macierz2]
```

*trace of a matrix – a sum of diagonal elements

Spin coupling

Anisotropic spin-spin interactions – those terms of the spin Hamiltonian that are not invariant under rotation in spin space (unaccompanied by rotation in real space) [13]

Compare two states:

•one spins point in +z direction and the other one in -z direction; both spins are on y-axis:

$$S_1^x=0,\quad S_1^y=0,\quad S_1^z=1;\quad S_2^x=0,\quad S_2^y=0,\quad S_2^z=-1;\qquad \hat{r}_x=0,\quad \hat{r}_y=1,\quad \hat{r}_z=0$$

•as above but both spins (not spinors) are rotated by 90 Deg about x-axis

$$S_1^x=0,\quad S_1^y=1,\quad S_1^z=0;\quad S_2^x=0,\quad S_2^y=-1,\quad S_2^z=0;\qquad \hat{r}_x=0,\quad \hat{r}_y=1,\quad \hat{r}_z=0$$

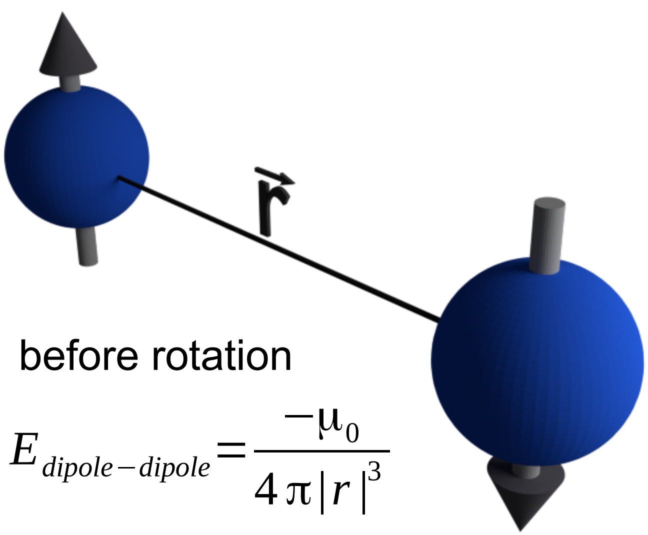

before rotation

$$E_{dipole-dipole}=\frac{-\mu_0}{4\pi|r|^3}$$

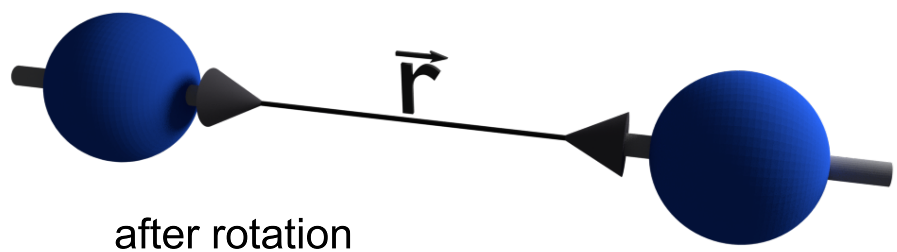

after rotation

$$E_{dipole-dipole}=\frac{\mu_0}{2\pi|r|^3}$$

The energies obtained in both cases are different – dipole-dipole interaction is anisotropic

Micromagnetism

- Micromagnetism*, as a refinement of *domain theory*, begins in 1930ies (Landau, Lifshitz) [9].
- In most cases of interest the use of atomistic description is too computationally demanding.
- In micromagnetism microscopic details of the atomic structure are ignored and the material is considered from the macroscopic point of view as **continuous** [9].
- Spins are replaced by classical vectors motion of which is described by LLG equation

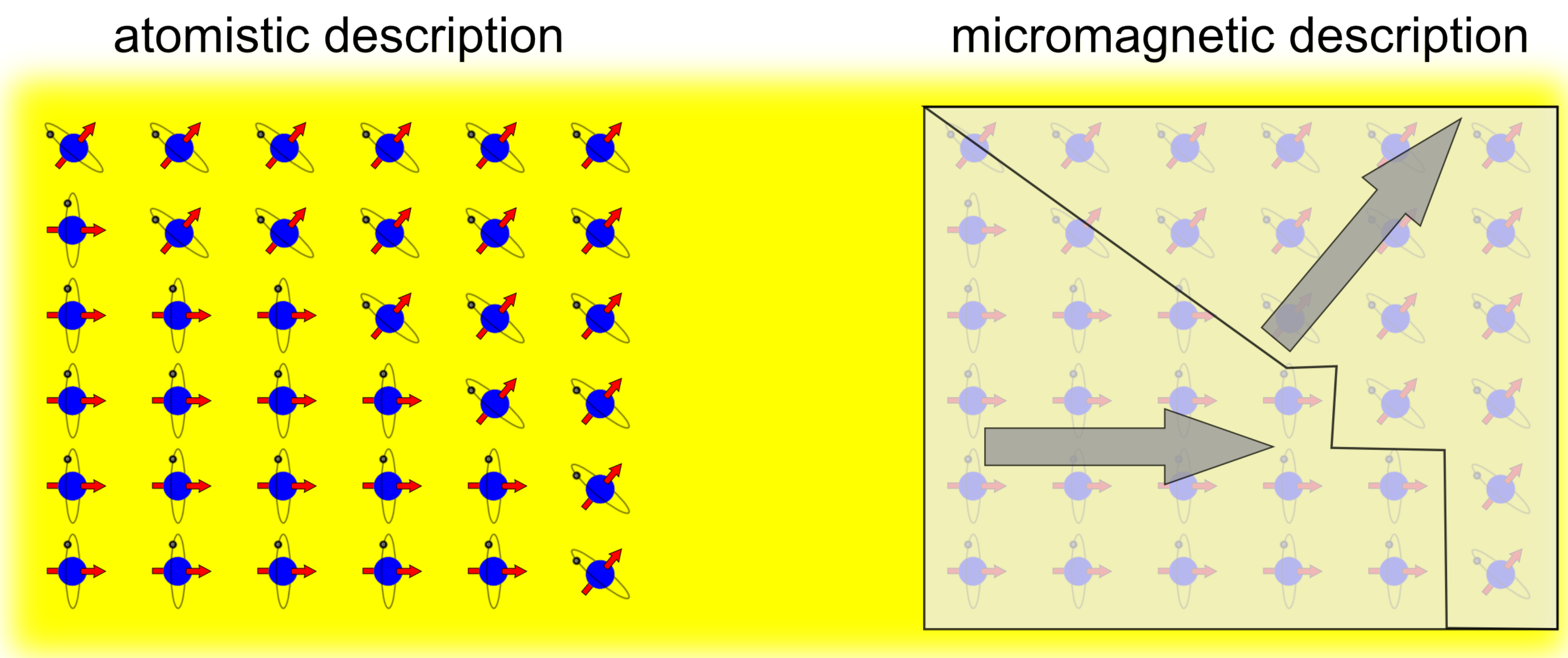

*the term micromagnetism was coined by William Fuller Brown

Continuous form of exchange energy

- The exchange energy among spins*, assuming that coupling is non-zero between nearest neighbors only, can be written as [9]:

$$E_{ex}=-JS^2\sum_{neighbours}\cos\phi_{i,j}$$

- The angles between the magnetic moments of neighboring spins are always small due to high strength of exchange coupling [8]. The angle between spins can be expanded in series coefficients**. In one dimensional case we have:

$$E_{ex}=-JS^2\sum_{neighbours}\cos\phi_{i,j}=-JS^2\sum_{neighbours}\left(1-\frac{1}{2}\phi_{i,j}^2+\ldots\right)\approx-JS^2\sum_{neighbours}1+JS^2\sum_{neighbours}\frac{1}{2}\phi_{i,j}^2$$

- If we use the state with all spins aligned ($\varphi_{ij}=0$) as a reference state we get:

$$E_{ex}\approx\frac{1}{2}JS^2\sum_{neighbours}\phi_{i,j}^2$$

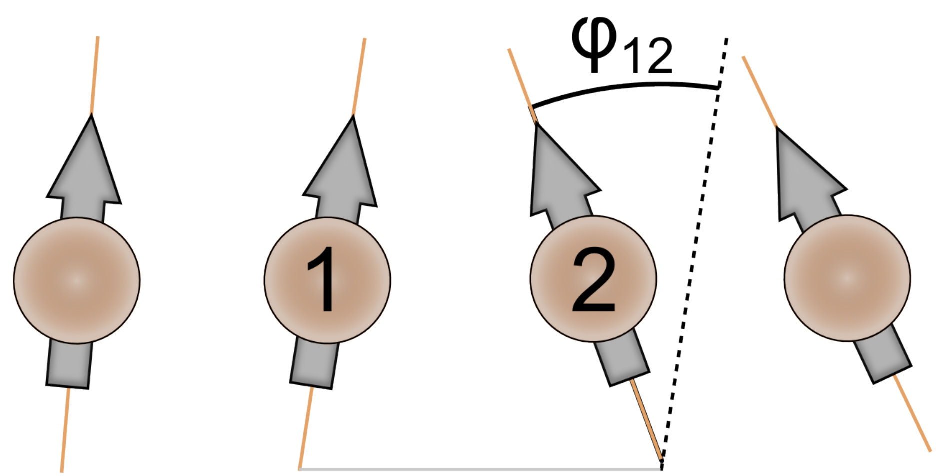

*this section is taken mainly from A. Aharoni, Introduction to the Theory of Ferromagnetism, Clarendon Press, Oxford 1996
**compare Bloch wall profile calculation in lecture 6

Continuous form of exchange energy

•If the angle between neighboring magnetic moments is small it can be expressed as:

$$|\phi_{i,j}| \approx |\vec{m}_i - \vec{m}_j|$$

$$\vec{m} := \frac{\vec{M}}{|\vec{M}|}$$

•If ***M*** (magnetization vector) is a continuous variable we can use first-order expansion in Taylor series [9] to get Δ**m** dependence on *r* :

$$|\vec{m}_i - \vec{m}_j| = \left| \left(dr_x \frac{\partial}{\partial x} + dr_y \frac{\partial}{\partial y} + dr_z \frac{\partial}{\partial z} \right) \vec{m} \right| = |(\vec{dr} \cdot \nabla) \vec{m}|$$

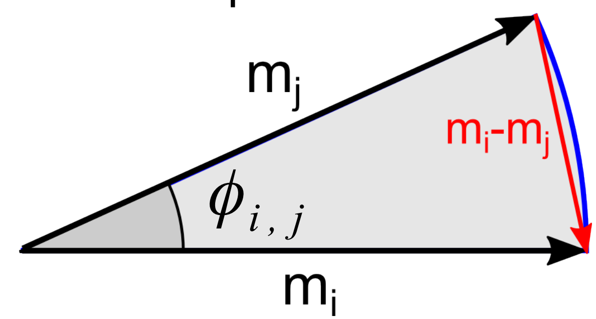

If φ_{ij} is small the vector $\mathbf{m_i}$-$\mathbf{m_j}$ is approximately of the same length as arc.

•The exchange energy then becomes:

$$E_{ex} \approx \frac{1}{2} J S^2 \sum_{neighbours} \phi_{i,j}^2 \approx \frac{1}{2} J S^2 \sum_i \sum_{\vec{dr}_i} \left| (\vec{dr} \cdot \nabla) \vec{m} \right|^2$$

summation from lattice point to all its neighbors

Continuous form of exchange energy

•As an example consider a simple cubic lattice with following six vectors to the nearest neighbors:

$$\vec{dr}: (1,0,0),\ (0,1,0),\ (-1,0,0),\ (0,-1,0),\ (0,0,1),\ (0,0,-1)$$

•We substitute the above vectors into the sum from previous page. We have:

$$\sum_{\vec{dr}_i} \left|(\vec{dr}\cdot\nabla)\vec{m}\right|^2 = 2\left(\frac{\partial}{\partial x}m_x\right)^2 + 2\left(\frac{\partial}{\partial y}m_x\right)^2 + 2\left(\frac{\partial}{\partial z}m_x\right)^2 + 2\left(\frac{\partial}{\partial x}m_y\right)^2 + 2\left(\frac{\partial}{\partial y}m_y\right)^2 + 2\left(\frac{\partial}{\partial z}m_y\right)^2 + 2\left(\frac{\partial}{\partial x}m_z\right)^2 + 2\left(\frac{\partial}{\partial y}m_z\right)^2 + 2\left(\frac{\partial}{\partial z}m_z\right)^2$$

$$\left(\frac{\partial}{\partial x}m_y\right)^2 + 2\left(\frac{\partial}{\partial y}m_y\right)^2 + 2\left(\frac{\partial}{\partial z}m_y\right)^2 = (\nabla m_y)\cdot(\nabla m_y)$$

$$\frac{1}{2}\sum_{\vec{dr}_i} \left|(\vec{dr}\cdot\nabla)\vec{m}\right|^2 = (\nabla m_x)^2 + (\nabla m_y)^2 + (\nabla m_z)^2$$

•Changing the summation to integration over the ferromagnetic body we obtain for cubic systems [9,14 p. 134]:

$$E_{ex} = \frac{1}{2} C \int \left[(\nabla m_x)^2 + (\nabla m_y)^2 + (\nabla m_z)^2 \right] dV$$

C - constant

•For lower symmetries of crystal lattice the expression for exchange energy density has slightly different forms . *"But for most cases of any practical interest this equation can be taken as a good approximation for the exchange energy, in as much as the assumption of the continuous material is a good approximation to the physical reality."*-A. Aharoni [9]

Continuous form of exchange energy

•Constant C depends on lattice type [9]:

$$E_{ex}=\frac{1}{2}C\int\left[(\nabla m_x)^2+(\nabla m_y)^2+(\nabla m_z)^2\right]dV$$

•For hexagonal crystal, such as cobalt, one obtains the same form of expression but the value of constant C is different:

$$C=\frac{4\sqrt{2}JS^2}{a}$$, where **a** is nearest neighbors' distance

•It is common ([8] for example) to write the expression for exchange energy density without the factor ½; a different constant A= ½ C is defined then.

•Both A and C are referred to as "**exchange constant of the material**" [9] or *exchange stiffness constant* (A) [8].

•Constant A is of the order of 10×10^{-12} Jm^{-1} in ferromagnetic materials.

•The exchange constant is roughly proportional to Curie temperature [15]:

$$A\approx\frac{k_B T_C}{2a_0},$$

a_0 -lattice parameter in a simple structure

$$C=\frac{2JS^2}{a}c$$

J- exchange integral, S – spin, a-lattice constant, c- constant

lattice	c
sc	1
bcc	2
fcc	4

	A[pJ m^{-1}]*
α-Fe	21
Co	31
Ni	7
$Ni_{80}Fe_{20}$ [7]	11

*from H. Kronmüller, M. Fähnle, Micromagnetism... [8]

Equilibrium condition

•From lecture 7/2012 we have the expression for the effective field [7, 9]:

$$\vec{H}_{eff}=\frac{2A}{M^2}\left[(\nabla M_x)^2+(\nabla M_y)^2+(\nabla M_z)^2\right]+\vec{H}_{app}+\vec{H}_d+\frac{\partial}{\partial\vec{m}}E_{anisotropy}$$

Effective field is an extension of magnetostatic energy terms of different origin:

$$E_{magn}=-\vec{M}\cdot\vec{B}$$

$$\vec{H}_{eff}=-\frac{1}{\mu_0 M_S}\frac{\partial}{\partial\vec{m}}E_{total}$$

•If one is interested in magnetization distribution static equilibrium the only condition that must be satisfied is [7,14]:

$$\vec{m}\times\vec{H}_{eff}=0$$

M must point at each point along the direction of the effective field

•Symmetry breaking of exchange interactions at outer surfaces brings additional so called *free boundary conditions* [7,14 p.135]:

$$\frac{\partial\vec{m}}{\partial\vec{n}}=0$$

to be read as $\frac{\partial}{\partial\vec{m}}f=\hat{x}\frac{\partial}{\partial m_x}f+\hat{y}\frac{\partial}{\partial m_y}f+\hat{z}\frac{\partial}{\partial m_z}f$ ([9, p.178], [14, p. 126])

Finite difference micromagnetism

•In the so called *field based approach* [7] one is seeking a numerical solution to LLG equation by first calculating the effective field and then inserting it into LLG equation.

$$\vec{H}_{eff} = -\frac{1}{\mu_0 M_S} \frac{\partial}{\partial \vec{m}} E_{total}$$

•The most difficult task is the calculation of long range magnetostatic interactions
• Exchange interactions and magnetocrystalline anisotropy are calculated locally:
- exchange energy depends on the magnetic moment orientation of nearest neighbors (nn) (6-neighbor exchange in simple cubic crystals) or nnn
- magnetocrystalline energy depends only on the orientation of the moment itself

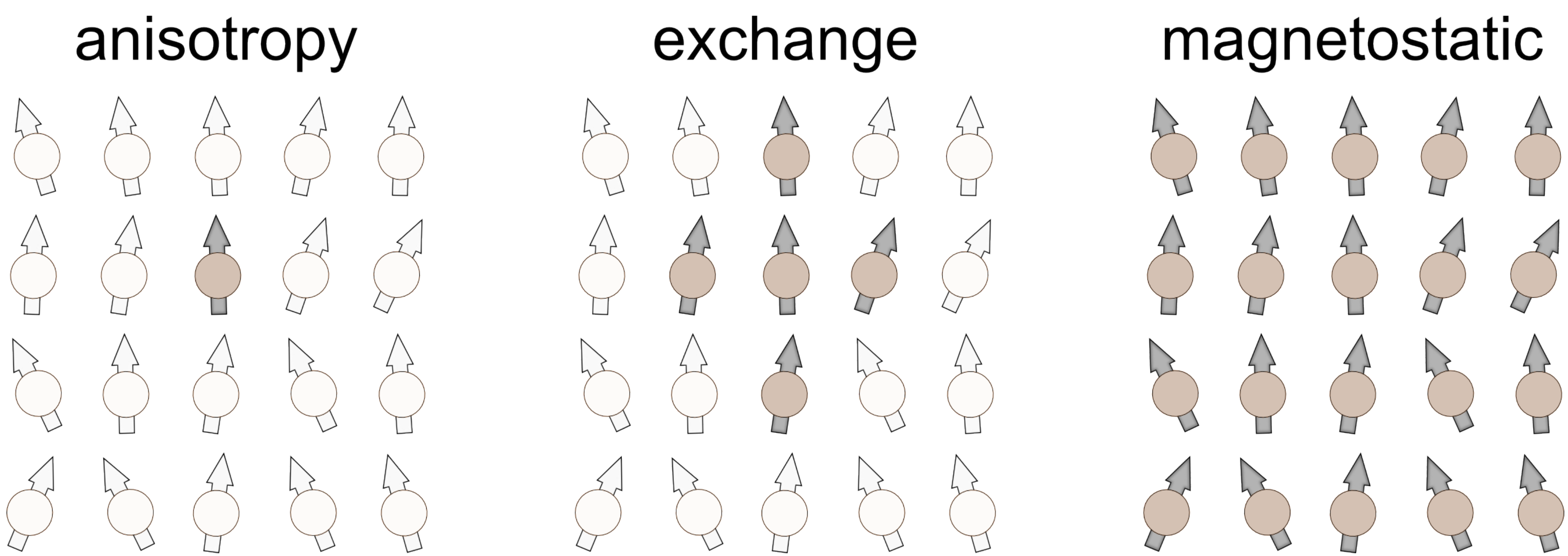

Finite difference micromagnetism – demagnetizing field evaluation

- Demagnetizing field evaluation can be calculated in formalism of volume and surface charges (lecture 2).
- **The volume of magnetic body is divided into a number of discretization cells.**
- It can be assumed that each cell has *constant* magnetization divergence within its volume and surface tiles with magnetic charge density [14].
- The demagnetizing field in a given cell is averaged across its volume for integrating LLG equation.
- It can be assumed too that the magnetization within each cell is homogeneous [8].
- The discretization cell must not necessarily be a cube [16].

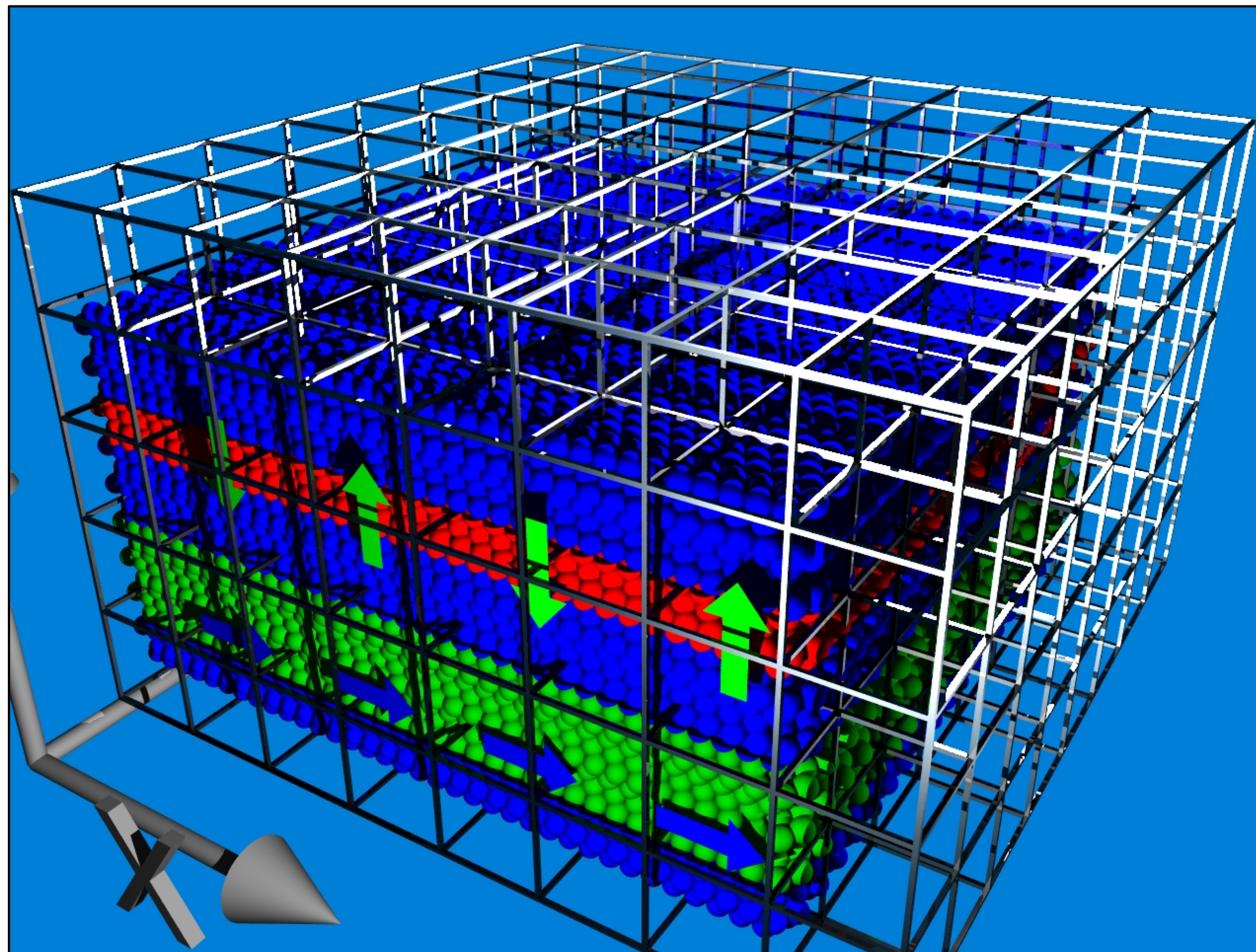

Finite difference micromagnetism – exchange lengths

•The required resolution of discretization (the maximum sizes of cells) is determined by the smallest features which may appear in the solution of micromagnetic problem [17].
•In micromagnetism there are three typical length scales [7,8]:

-magnetocrystalline exchange length – related to the width of the Bloch wall ($\pi\, l_k$)

$$l_k = \sqrt{A/K_1}$$

-magnetostatic exchange length* [10] – related to the width of the Néel wall ($\pi\, l_s$)

$$l_k = \sqrt{\frac{2A}{\mu_0 M_s^2}}$$

-thermal exchange length [13]

$$l_k = \sqrt{\frac{A}{\mu_0 M_s H_{th}}}, \qquad H_{th} = \sqrt{\frac{2\alpha k_b T}{\Delta \gamma \mu_0 M_s l^3}}$$

• The discretization cell should be smaller than the smallest of three lengths defined above [17].
•The magnetostatic exchange length rarely exceeds a few nanometers in 3d ferromagnetic metals or alloys; it imposes a severe constraint on the mesh size in numerical simulations [7].

*that length is sometimes defined without ,,2” under square root [7].

Finite difference micromagnetism – exchange lengths

•The magnetostatic exchange length rarely exceeds a few nanometers in 3d ferromagnetic metals or alloys; it imposes a severe constraint on the mesh size in numerical simulations [7].

	l_k[nm]	l_s[nm]
α-Fe	21	3.3
Co	8.3	4.9
Ni	7	8.7
$SmCo_5$	0.84	5.3

table data from:
H. Kronmüller, M. Fähnle, Micromagnetism and the Microstructure of Ferromagnetic Solids, Cambridge University Press, 2003

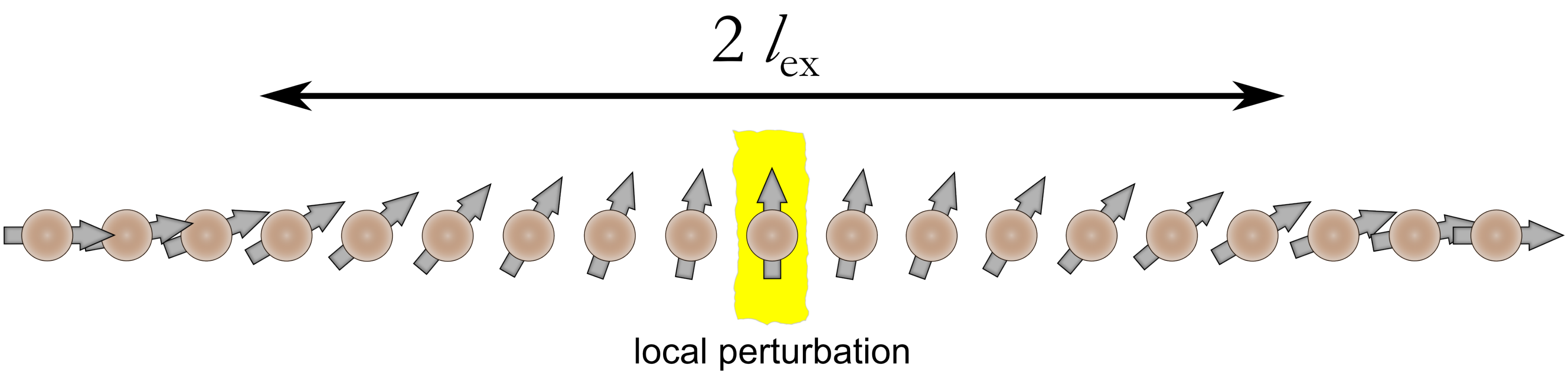

•At a distance roughly equal to the appropriate exchange length the spin configuration is that of unperturbed state:
- the local perturbation can be a grain with high magnetocrystalline anisotropy with easy direction perpendicular to the applied field (here, on the drawing, directed to the right)
-it can be laser-heated region of the sample in which magnetocrystalline anisotropy vanishes and the spin is directed along the external field (this time directed upward), etc.

Finite difference micromagnetism – exchange lengths

- •In micromagnetic simulation every discretization cell interacts with every other cell by magnetostatic interactions .
- •The shortest exchange length determines which energy term contributes the largest amount to the total energy [8].
- •In soft magnetic materials the spin arrangements are more or less divergence free – **pole avoidance principle** [9].

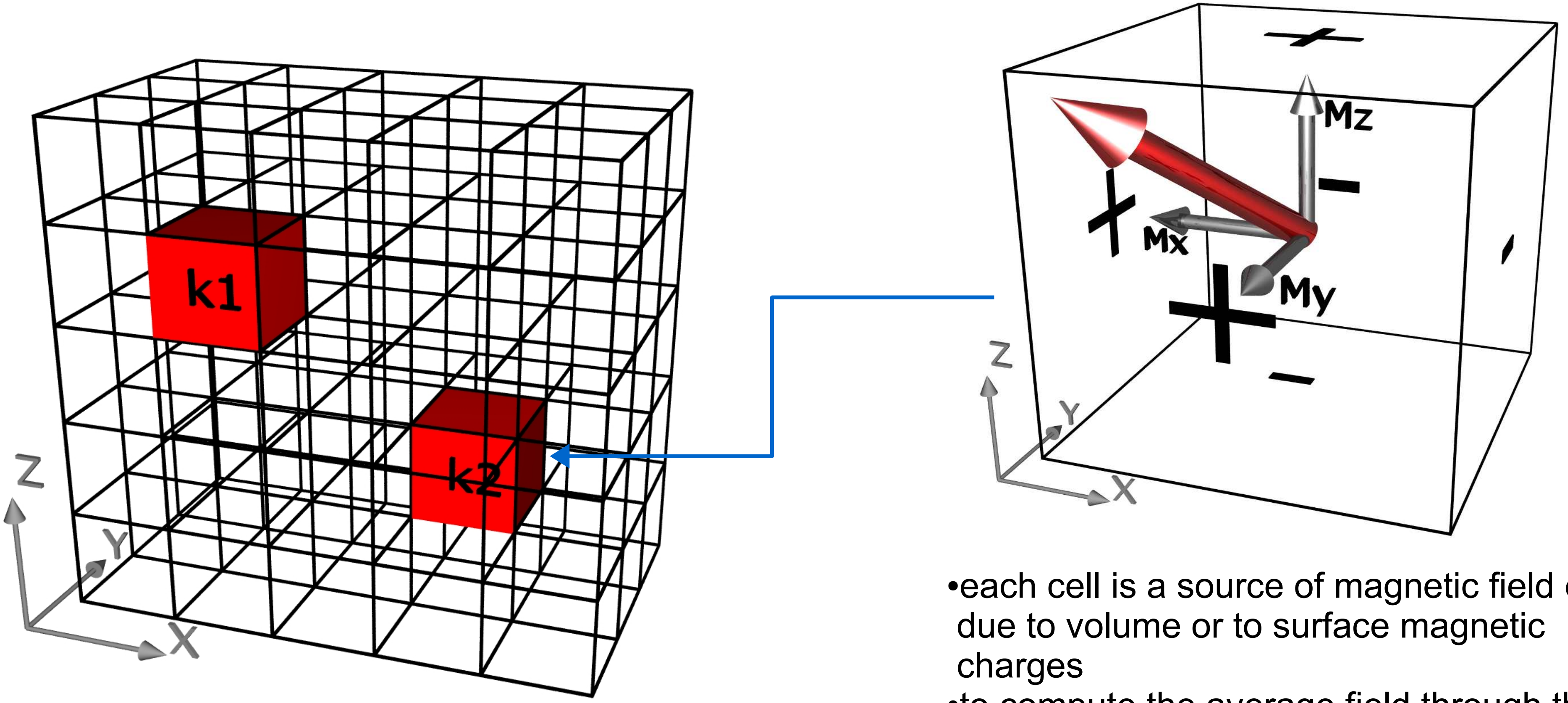

- •each cell is a source of magnetic field either due to volume or to surface magnetic charges
- •to compute the average field through the cell the demagnetizing factors for rectangular ferromagnetic prisms are used.

Finite difference micromagnetism – calculation scheme

- In dynamic micromagnetic simulation the effective field is calculated as the input of LLG equation (for example OOMMF) [18].
- The magnetic moments of the cells are then updated according to angular velocities obtained from LLG equation.
- The time step is adjusted so that the "*the total energy of the system decreases, and the maximum error between the predicted and final M is smaller than a nominal value*" [18]

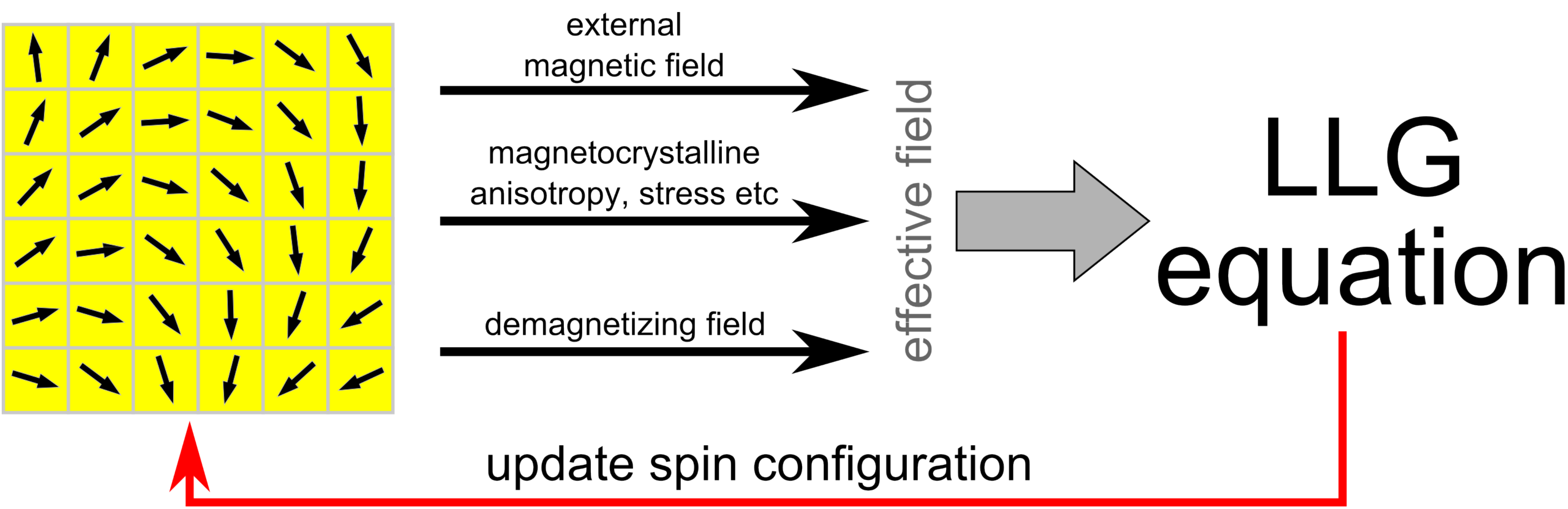

$$\frac{d\vec{m}}{dt} = \frac{\gamma}{(1+\alpha^2)} \vec{m} \times \vec{B} - \frac{\alpha}{(1+\alpha^2)} \frac{\gamma}{|\vec{m}|} \vec{m} \times \vec{m} \times \vec{B}$$

Finite difference micromagnetism – an example

•Remanent state of thin 900×900nm NiFe film; discretization cell 3×3×1nm^3
•Simulation time – 6ns (simulated with OOMMF [18])

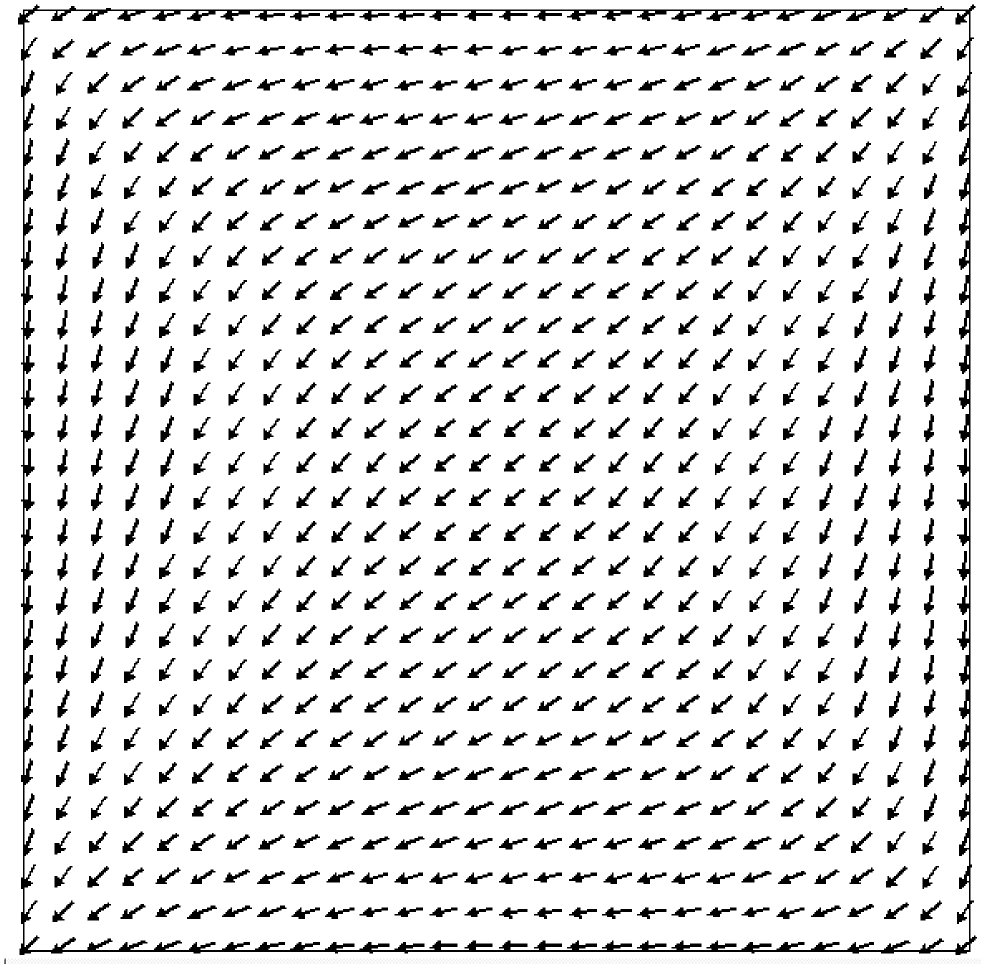

each arrow corresponds to 11×11 discretization cells

•Magnetization tends to be align along outer edges of the specimen – minimization of surface charges
•Exchange anisotropy forces moments to be parallel to each other – central part of the specimen

Spintronic devices

Spin-torque wave generators*
In 1996 J. Slonczewski predicted that the current flowing between two ferromagnetic layers may induce a steady precession of the moments or novel form of switching of magnetization [20]. The latter effect has already found application in STT-MRAM. The first effect is, among others, being investigated with a hope of fabricating novel microwave generators [21].

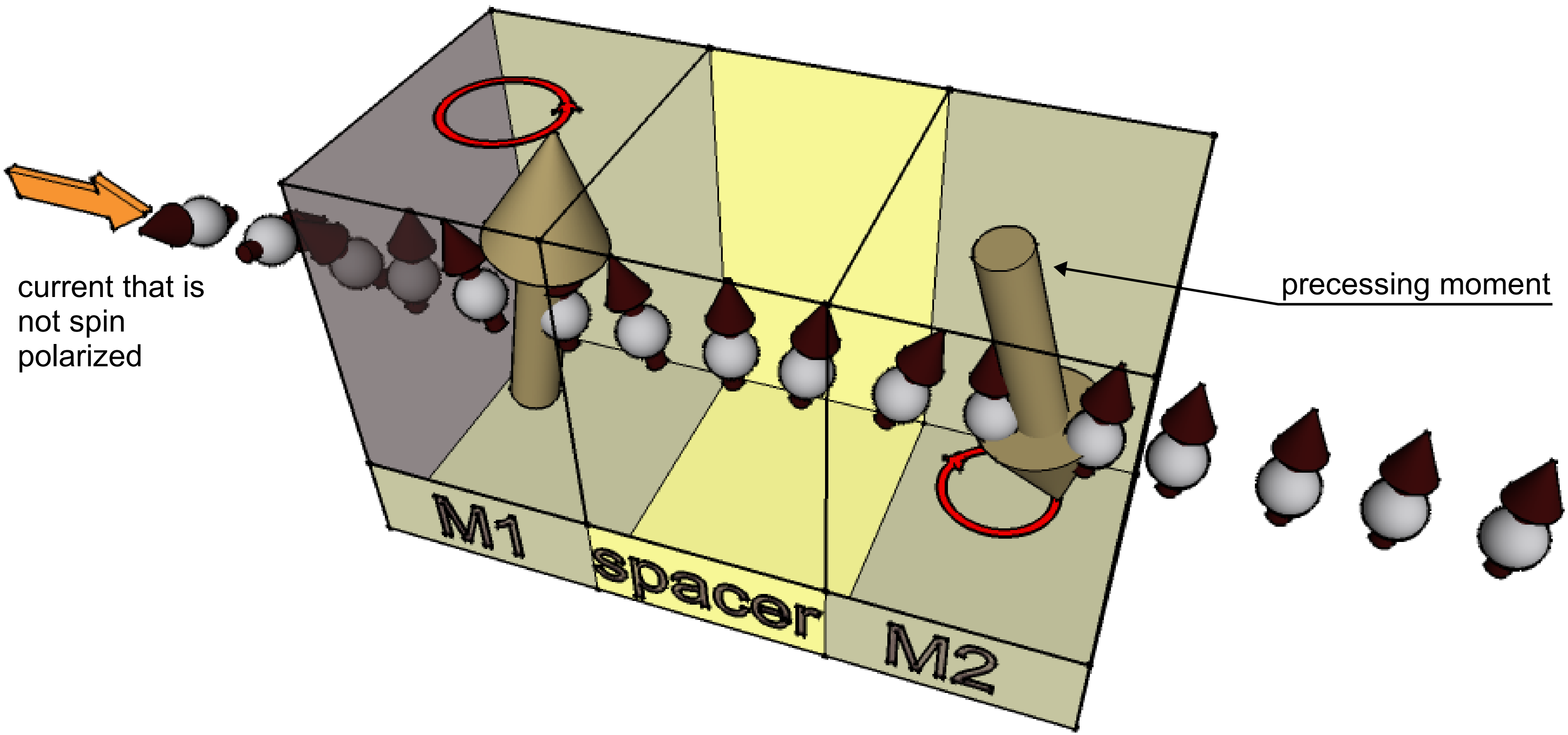

*STO – Spin Torque Oscillator

Spintronic devices

Landau-Lifshitz-Gilbert (LLG) equation with spin torque

- by including an additional term LLG equation can be extended to fenomenologically describe the influence of spin polarized current on magnetization dynamics [20,22,23]
- in the simplest case of two magnetic layers, with magnetic moment of one of them fixed the motion of magnetic moment can be approximately given by the equation [22]:

$$\frac{d\vec{m}_{free}}{dt} = -\mu_0 \gamma \vec{m}_{free} \times \vec{H}_{eff} - \mu_o \gamma \alpha \vec{m}_{free} \times (\vec{m}_{free} \times \vec{H}_{eff}) + \frac{\varepsilon J_{injected} \hbar}{e l_z 2} \frac{\gamma}{M_{s1}} m_{free} \times (\vec{m}_{free} \times \vec{m}_{fix})$$

ε -current polarization

l_z -thickness of the free layer

$J_{injected}$ -current density (of the order of 10^{10}-10^{11} Am^{-2})

M_{s1} -magnetization of the free layer

Note that spin-current injection can result in the spin-waves generation especially in nanocontact configuration where the area into which spin current is being pumped is coupled by the exchange interaction with the rest of the film [22]

nanopillar

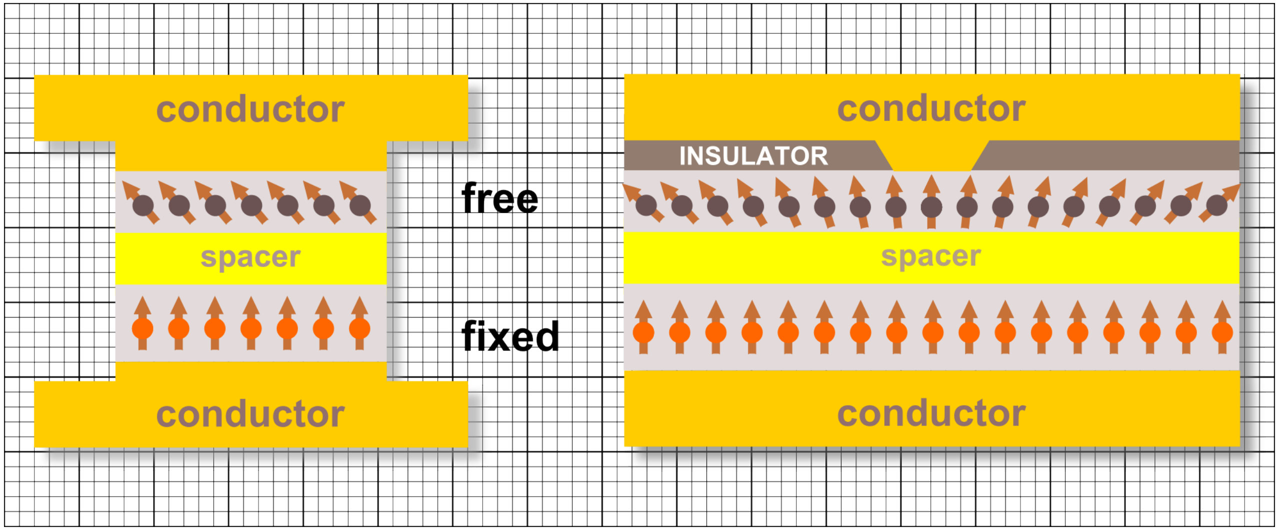

nanocontact [22]

- spin waves
- lower FWHM of emitted power
- edge deffects associated with patterning are mitigated
- no parasitic dipolar coupling between free and fixed layer

Spintronic devices

Switching of thin film magnetic moment - macrospin approximation

- one magnetic moment under combined influence of magnetic field and spin-polarized currrent [19]

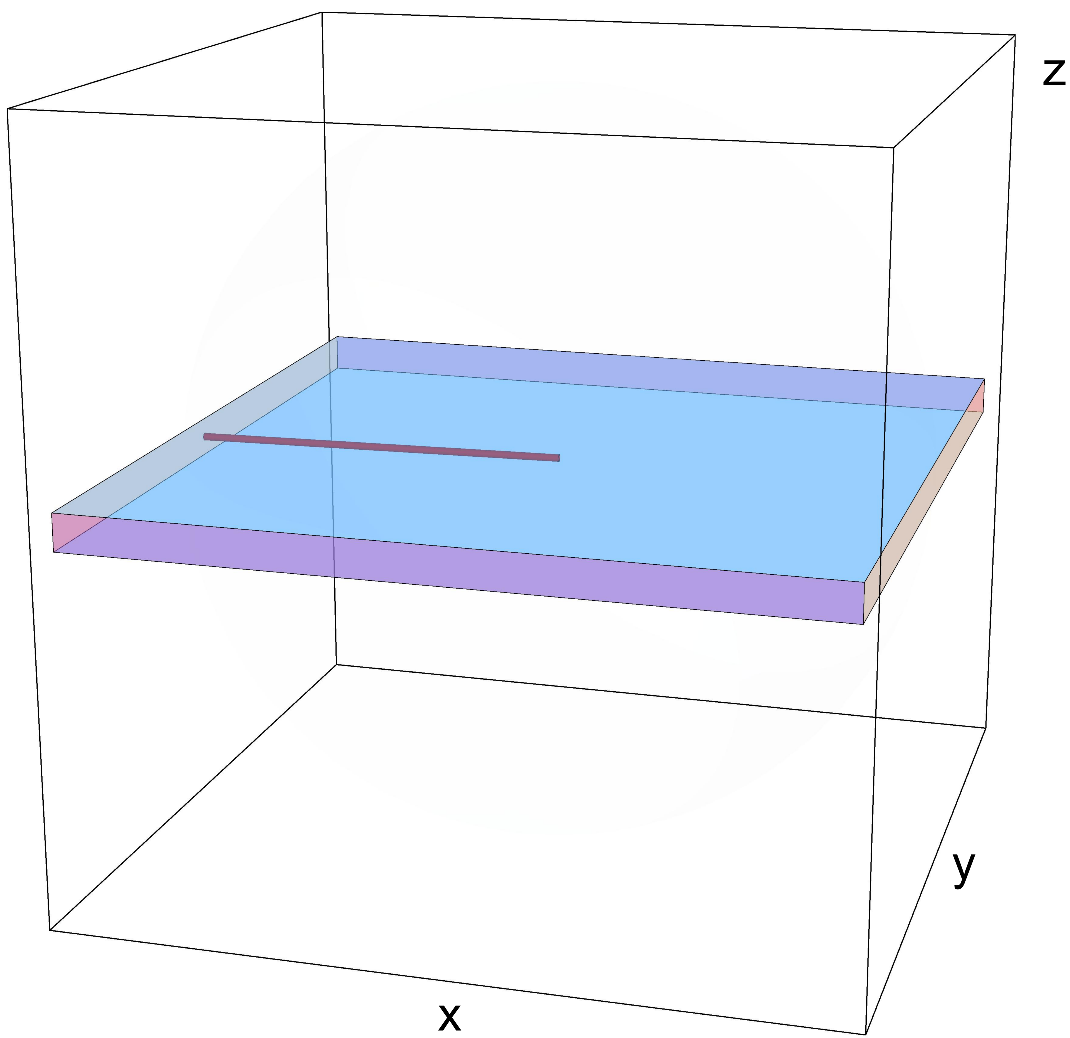

- the magnetic moment (red line) points initially in (-0.95,-0.05,0) direction (if it pointed exactly in -x direction it would not reverses under the action of the field directed in +x direction*)

- thin film is infinite in the x,y-plane so the moment experiences shape anisotropy with demagnetizing field, equal to z-component of magnetization, which tends to keep the moment in the plane of the film

*in real films thermal fluctuations and spin deviations due to magnetostatic fields are enough to initiate the reversal

Spintronic devices

Switching of thin film magnetic moment - macrospin approximation

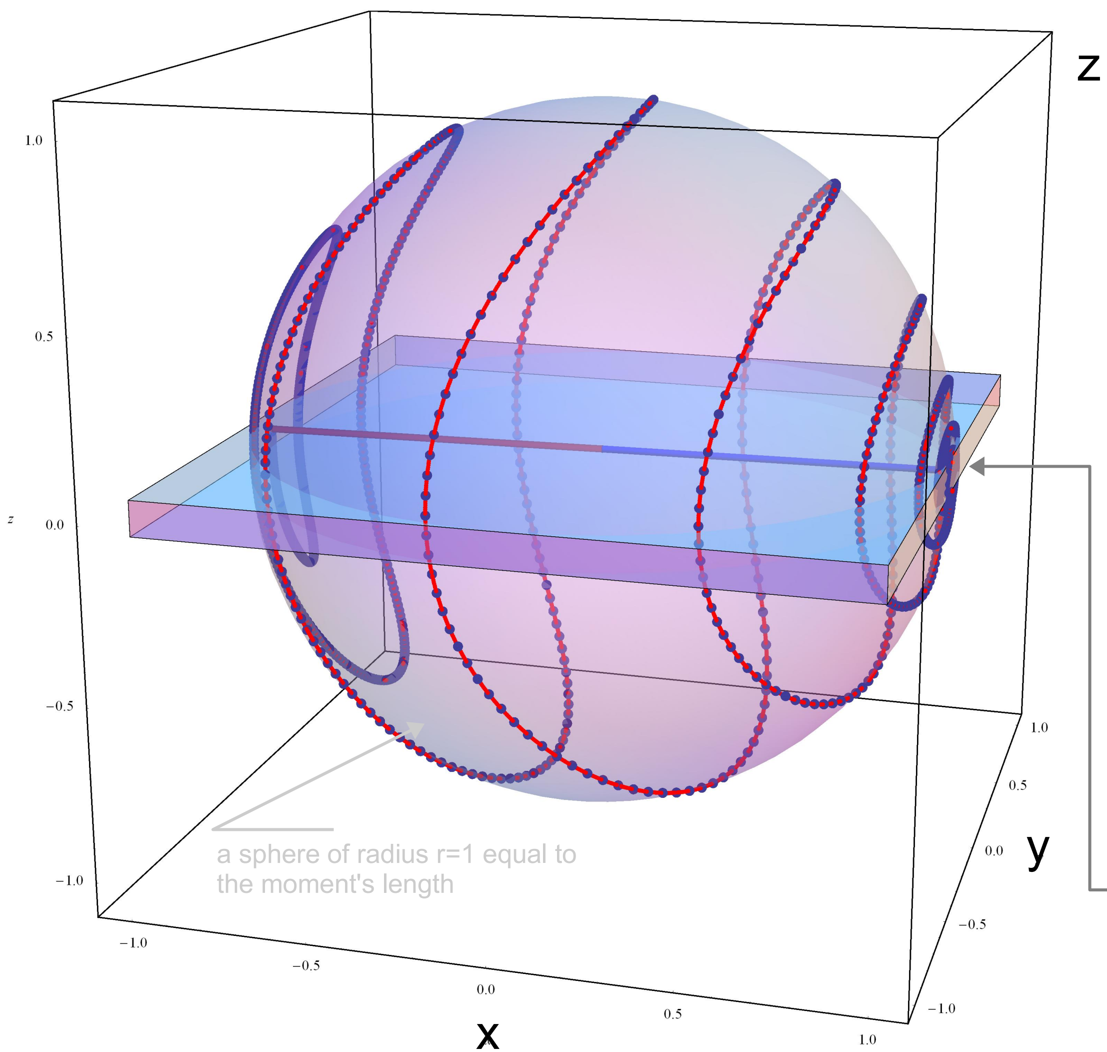

- after (instantaneous) application of the field in +x direction the moment precesses to its final position (blue line)

- blue dots mark equal time intervals dt
- parameters:

initial moment direction: (-0.95,-0.05,0)
H=(1,0,0)
damping =0.1
current=0
saturation reached* after 13436 dt

*after which time step (all steps equal) the magnetic moment for the first time points along the field direction to within 1 deg of arc

Spintronic devices

Switching of thin film magnetic moment - macrospin approximation

Mathematica 6 code to get the previous and following graphs:

first evaluate the first cell and do not worry about "*Part specification Mi[[1]] is longer than depth of object.*" etc.

```
ClearAll[Mi,Hx,Hy,Hz,Current,alfa,anizo,S];
M={Mi[[1]],Mi[[2]],Mi[[3]]};
Spin={S[[1]],S[[2]],S[[3]]};
He={Hx,Hy,Hz-anizo Mi[[3]]};(*thin film-arbitrary field direction*)(*anizo=1 - cienkawarstwa; anizo=0 - isotropic sphere - no magnetic anisotropy*)

Md=Sqrt[M.M];
 dMtodt=- Cross[M,He] - alfa  Cross[M, Cross[M, He]]+Current  Cross[M,Cross[M,Spin]];(*this gives the set of equation describing time evolution of the magnetic moment orientation
which I have inserted into the k-loop below*)
```

———————————————————— cell border

then evaluate the second cell; to get the graph for other parameters (damping, field direction, current etc.) the first cell needs not to be evaluated again

```
  ilepunktow=14000;(*number of points- time intervals*)
orientacjamomentu=Table[{0,0,0},{i,1,ilepunktow-1}];
dt=0.01;(*time step*)
alfa=0.1;
anizo=1; (*anizo=0;-sphere*)
Hvalue=1;(*field value*)
Hx=1;(*components relative*)
Hy=0;
Hz=0;
Ha=Sqrt[Hx^2+Hy^2+Hz^2]/Hvalue;
Hx=Hx/Ha;
Hy=Hy/Ha;
Hz=Hz/Ha;

Mi={-0.95,-0.05,0};(*initial moment orientation*)
moment=Sqrt[Mi.Mi];(*moment's length*)
Mi=Mi*(1/moment);
Current=0; (*current*)
(*spin-current orientation:*)
S={-1,0,0};

wy3=Graphics3D[{RGBColor[1,0,0],Cylinder[{{0,0,0},1*{Mi[[1]],Mi[[2]],Mi[[3]]}},0.01]}];(*line of initial moment orientation*)

licznik=0;

gamma=2;
timemultiplier=1/(moment gamma (1+alfa^2));

coile=10;(*co ile punktow stawiac marker*)
macierzznacznikow=Table[{0,0,0},{i,1,Floor[ilepunktow/coile]-1}];
licznik=1;
l=1;
pp=0;(*print only once*)
For[k=1,k<ilepunktow,k++,

 Mi[[1]]=Mi[[1]]+dt timemultiplier dMtodt[[1]];
 Mi[[2]]=Mi[[2]]+dt timemultiplier dMtodt[[2]];
 Mi[[3]]=Mi[[3]]+dt timemultiplier dMtodt[[3]];

 (*adjust the M length - to take care of numeric errore:*)
 temp=Sqrt[Mi.Mi];
 Mi[[1]]=Mi[[1]]/temp;Mi[[2]]=Mi[[2]]/temp;Mi[[2]]=Mi[[2]]/temp;


 orientacjamomentu[[k,1]]=Mi[[1]];orientacjamomentu[[k,2]]=Mi[[2]];orientacjamomentu[[k,3]]=Mi[[3]];

 (*angle A between the moment and the field direction*)
 kos=(Mi[[1]]*Hx+Mi[[2]]*Hy+Mi[[3]]*Hz)/Hvalue;
 If[Abs[kos]>=0.999847 && pp==0,(*about 1 degree of arc*)
  {Print["Field direction reached after ",k, " dt"];
   pp=1;}
  ]


  (*the markers on the orbit are placed every coile-th iteration of k*)
  If[licznik<coile,licznik=licznik+1,{licznik=1;
   macierzznacznikow[[l,1]]=orientacjamomentu[[k,1]];
   macierzznacznikow[[l,2]]=orientacjamomentu[[k,2]];
   macierzznacznikow[[l,3]]=orientacjamomentu[[k,3]];

   l++}
  ]


]


wy1=ListPointPlot3D[orientacjamomentu, PlotRange->{{-1.1,1.1},{-1.1,1.1},{-1.1,1.1}}, BoxRatios->{1,1,1},AxesLabel->{x,y,z},PlotStyle->{Red},BoxStyle->Directive[Thickness[0.004]]];

wy4=ListPointPlot3D[macierzznacznikow, PlotRange->{{-1.1,1.1},{-1.1,1.1},{-1.1,1.1}},AxesStyle->{Thick}, BoxRatios->{1,1,1},PlotStyle->PointSize[Large],AxesLabel->{X,Y,Z},ImageSize->600,ViewPoint->{Pi,Pi/2,2}];
wy2=Graphics3D[{Opacity[0.3],Sphere[{0,0,0},1]}];
warstwa=Graphics3D[{Opacity[0.5],Cuboid[{1,1,0-0.05},{-1,-1,0.05}]}];
wy5=Graphics3D[{RGBColor[0,0,1],Cylinder[{{0,0,0},1*{Mi[[1]],Mi[[2]],Mi[[3]]}},0.01]}];(*final moment direction*)
wy3=Show[wy1,wy4,wy3,wy2,wy5,warstwa,ImageSize->800,ViewVector->{2,-7,2}(*relative to the center*),ViewCenter->{0.5,0.5,0.5},ImageMargins->20,BoxStyle->{AbsoluteThickness[4],RGBColor[0,0,0]}]
(*Export["D:\\yourfolder\\image.jpg",wy3,ImageResolution->300]*)
```

Spintronic devices

Switching of thin film magnetic moment - macrospin approximation

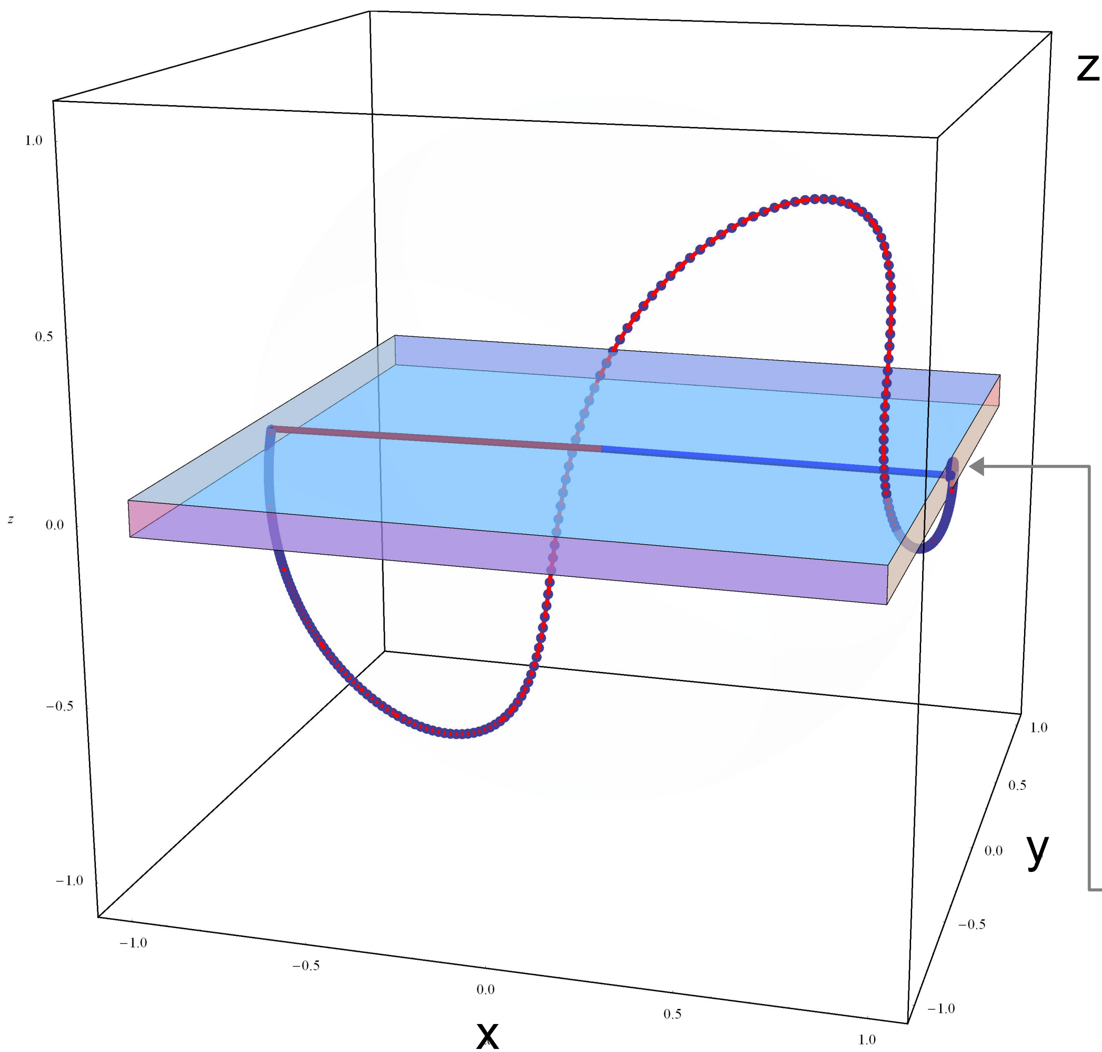

•after (instantaneous) application of the field in +x direction the moment precesses to its final position (blue line)

•blue dots mark equal time intervals dt
•parameters:

initial moment direction: (-0.95,-0.05,0)
H=(1,0,0)
damping =**0.5**
current=0
saturation reached* after **3140** dt – note that the moment switched in a shorter time in spite of higher damping constant

final position of the moment

*after which time step (all steps equal) the magnetic moment for the first time points along the field direction to within 1 deg of arc

Spintronic devices

Switching of thin film magnetic moment - macrospin approximation

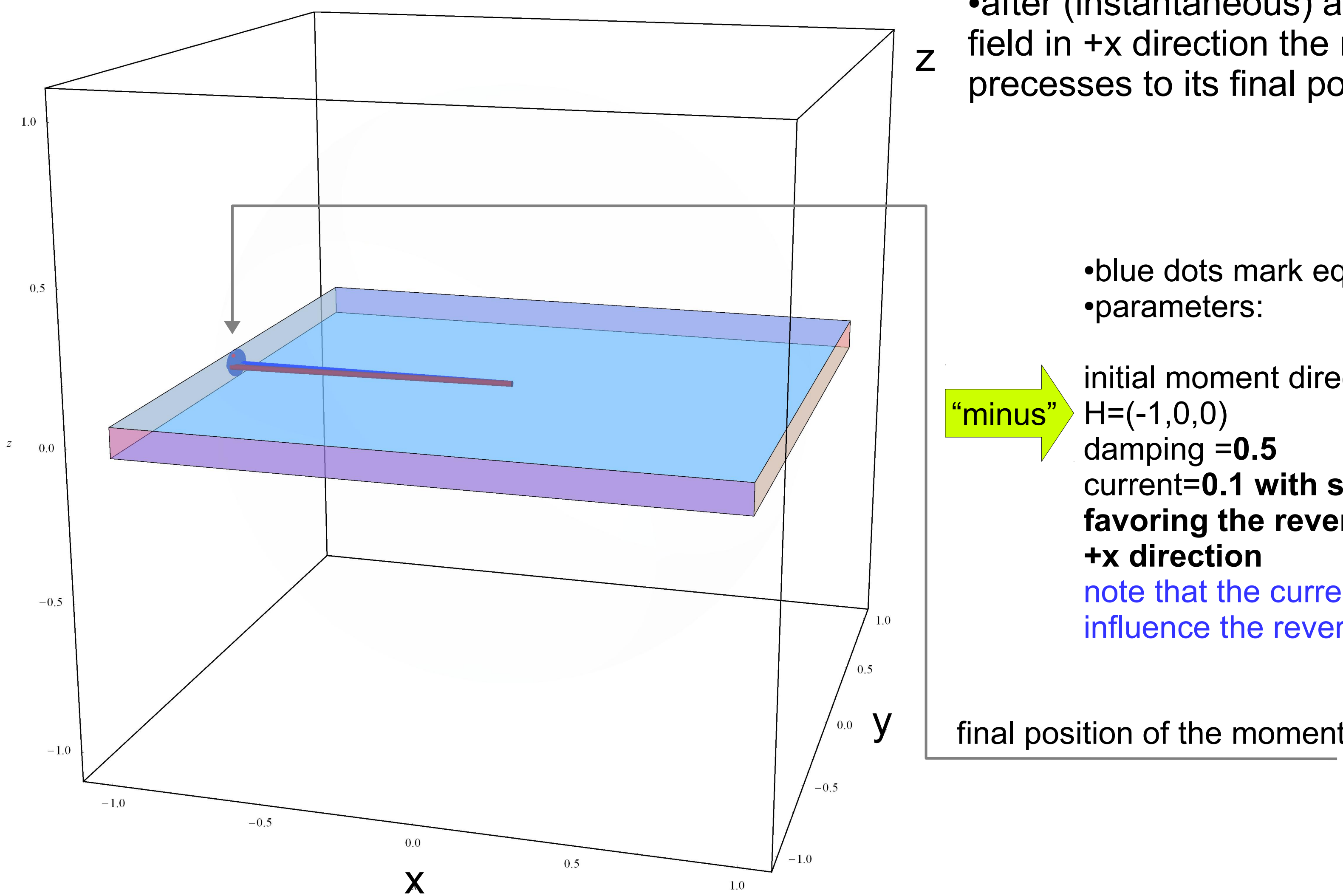

•after (instantaneous) application of the field in +x direction the moment precesses to its final position (blue line)

•blue dots mark equal time intervals dt
•parameters:

initial moment direction: (-0.95,-0.05,0)
H=(-1,0,0)
damping =**0.5**
current=**0.1 with spin orientation favoring the reversal of the moment to +x direction**
note that the current is too low to influence the reversal

Spintronic devices

Switching of thin film magnetic moment - macrospin approximation

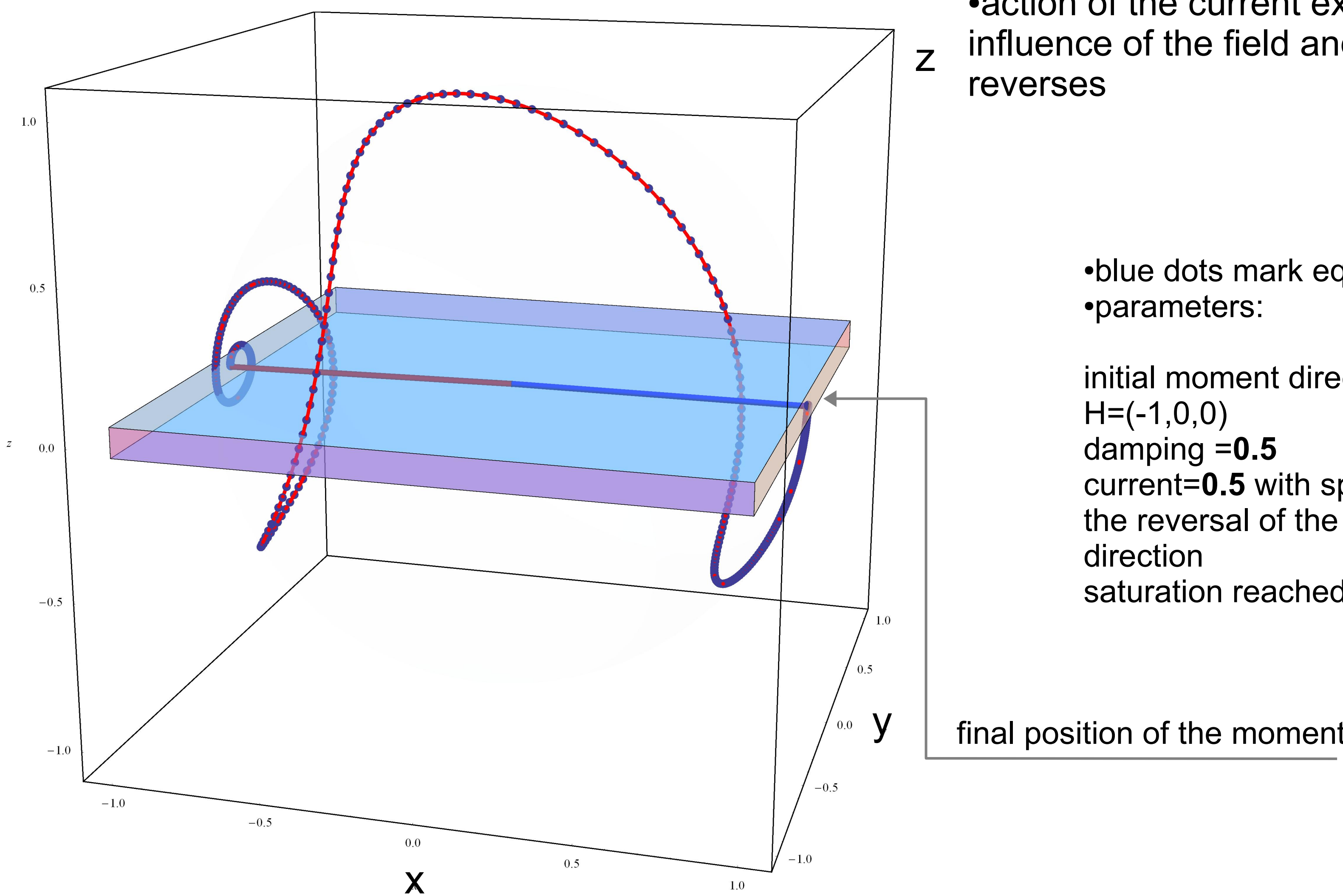

- action of the current exceeds the influence of the field and the moment reverses

- blue dots mark equal time intervals dt
- parameters:

initial moment direction: (-0.95,-0.05,0)
H=(-1,0,0)
damping =**0.5**
current=**0.5** with spin orientation favoring the reversal of the moment to +x direction
saturation reached* after **3846** dt

*after which time step (all steps equal) the magnetic moment for the first time points along the field direction to within 1 deg of arc

Spintronic devices

Switching of thin film magnetic moment - macrospin approximation

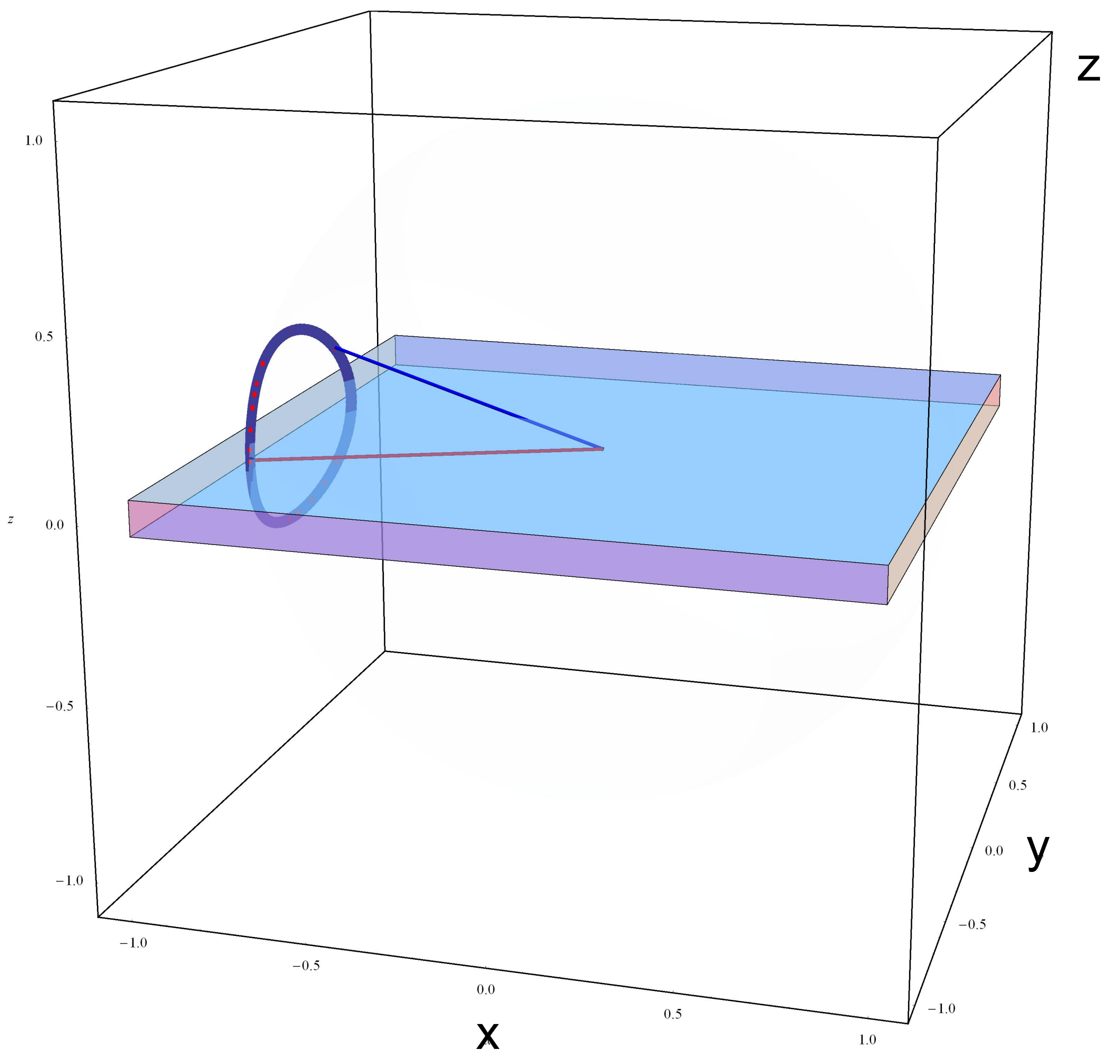

•the precession of magnetic moment can be used to generate microwaves through the effect of GMR [19]

•blue dots mark equal time intervals
•parameters:

initial moment direction: (-0.95,-0.4,0)
H=(-1,0,0)
damping =**0.5**
current=**0.149** with spin orientation favoring the reversal of the moment to +x direction
action of the current balances the damping and the moment performs steady precession

Spintronic devices

Spin-torque generators*
In 1996 J. Slonczewski predicted that the current flowing between two ferromagnetic layers may induce a steady precession of the moments or novel form of switching of magnetization [20]. The latter effect has already found application in STT-MRAM. The first effect is, among others, being investigated with a hope of fabricating novel mocrowave generators [21].

sputter-deposited multilayer stacks consisting of 2 nm CoFe (FM1)/4 nm Cu/4 nm CoFe (FM2)

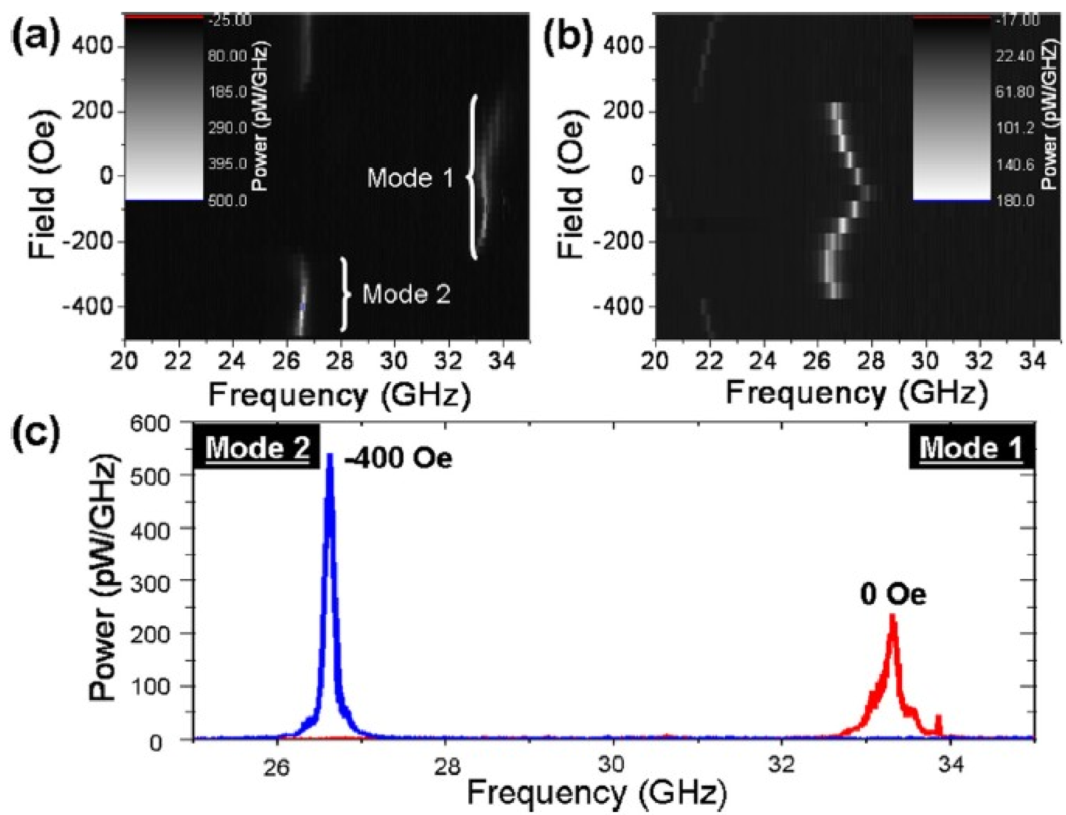

FIG. 2. High frequency phase diagram for STO device 1 (a) and device 2 (b) depicting the two field regimes corresponding to optical (mode 1) and acoustic (mode 2) oscillation modes for the two ferromagnets. (c) Power spectral density for the oscillator in (a) at 0 and −400 Oe, showing well defined spectral peaks with large output powers at different ultrahigh frequencies. The integrated powers of the spectral peaks are 72.4 pW at Ha = 0 Oe and 128.5 pW at Ha = −400 Oe, and we observe a hop of ~6.5 GHz between modes.

- bias current ~0.7mA
- both magnetic layers precess
- the precession and power generation is observed **in zero external magnetic field**

image from: P.M. Braganca, K. Pi, R. Zakai, J.R. Childress, B.A. Gurney, Applied Physics Letters **103**, 232407 (2013)

*STO – Spin Torque Oscillator

Magnetoresistive memory

***Everspin** Spin Torque MRAM Technology*

From company's press release* (2016, August):
•"Everspin Technologies strengthens its leadership position in MRAM by shipping the world's first product using **perpendicular magnetic tunnel junction** (pMTJ) based **ST-MRAM** to customers."

•256Mb

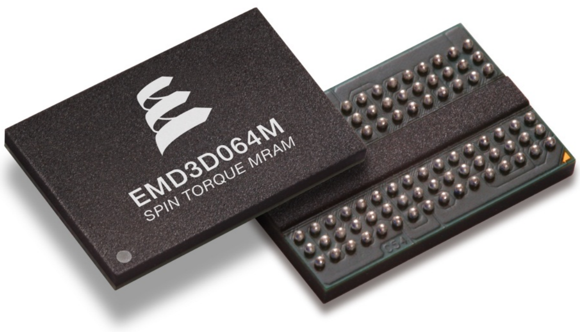

image from www.everspin.com/product-images

Example Data Sheet information (Everspin MR4A08B):

•Fast 35 ns read/write cycle

•**Unlimited** read & write endurance

•Data always non-volatile for >**20-years** at temperature (?)

*https://www.everspin.com/news/everspin-256mb-st-mram-perpendicular-mtj-sampling

Bibliography:

[1] A. Hubert, R. Schäfer, Magnetic domains: the analysis of magnetic microstructures, Springer 1998
[2] Р. Суху, Магнитные Тонкие Пленки, Издательство МИР Москва 1967
[3] W. Ketterle, MIT Physics 8.421 Atomic and optical Physics, http://cua.mit.edu/8.421_S06/
[4] M. Getzlaff, Fundamentals of Magnetism, Springer-Verlag Berlin-Heidelberg 2008
[5] H. Kronümller, General Micromagnetic Theory, in Handbook of Magnetism and Advanced Magnetic Materials, edited by H. Kronümller and S.S.P. Parkin, vol. 2, Wiley, 2007.
[6] T. Gilbert, IEEE Trans. Magn. **40**, 3443 (2004)
[7] J. Miltat and M. Donahue, Numerical micromagnetics: finite difference methods, in Handbook of Magnetism and Advanced Magnetic Materials, edited by H. Kronümller and S.S.P. Parkin, vol. 2, Wiley, 2007.
[8] H. Kronmüller, M. Fähnle, Micromagnetism and the Microstructure of Ferromagnetic Solids, Cambridge University Press, 2003
[9] A. Aharoni, Introduction to the Theory of Ferromagnetism, Clarendon Press, Oxford 1996
[10] K. Pasrij, S. Kumar, Phys. Rev. B, **88** 144418 (2013)
[11] K. Bergmann, A. Kubetzka, O. Pietzsch, R. Wiesendanger, J. Phys.:Condens. Matter **26** 394002 (2014)
[12] K.C. Border, *More than you wanted to know about quadratic forms*, v. 2016.10.20::14.05
[13] Ch. L. Henley, Spin Hamiltonians and Exchange interactions, 2007 (www.lassp.cornell.edu/clh/p654/MM-Lec0.pdf)
[14] W. F. Brown, Jr., Magnetostatic Principles in Ferromagnetism, North-Holland, Amsterdam 1962
[15] J.M.D. Coey, Magnetism and Magnetic Materials, Cambridge University Press 2009
[16] M. Kisielewski, A. Maziewski, T. Polyakova, V. Zablotskii, Physical Review B **69**, 184419 (2004)
[17] W. Scholz et al., Computational Materials Science **28**, 366 (2003)
[18] M. J. Donahue and D. G. Porter, OOMMF User's Guide, Version 1.0, Interagency Report NISTIR 6376, NIST, Gaithersburg, MD (Sept 1999), http://math.nist.gov/oommf/
[19] D.C. Ralph, M.D. Stiles, Journal of Magnetism and Magnetic Materials **320**, 1190 (2008); tutorial article!
[20] J.C. Slonczewski, JMMM **159**, L1 (1996)
[21] P.M. Braganca, K. Pi, R. Zakai, J.R. Childress, B.A. Gurney, Applied Physics Letters **103**, 232407 (2013)P.M. Braganca, K. Pi, R. Zakai, J.R. Childress, B.A. Gurney, Applied Physics Letters **103**, 232407 (2013)
[22] W.H. Rippard, M.R. Pufall, Microwave Generation in Magnetic Multilayers and Nanostructures, in Handbook of Magnetism and Advanced Magnetic Materials, edited by H. Kronümller and S.S.P. Parkin, vol. 2, Wiley, 2007
[23] D. Pinna, A.D. Kent, D.L. Stein, J. Appl. Phys. **114**, 033901 (2013)